Proceedings of the 4th BSME-ASME International Conference on Thermal Engineering
27-29 December, 2008, Dhaka, Bangladesh

EFFECT OF ENGINE SPEED ON PERFORMANCE OF FOUR-CYLINDER DIRECT INJECTION HYDROGEN FUELED ENGINE

M. M. Rahman, Mohammed K. Mohammed and Rosli Abu Bakar

Faculty of Mechanical Engineering, Universiti Malaysia Pahang
Tun Abdul Razak Highway, 26300, Gambang, Kuantan, Pahang, Malaysia
Email: mustafizur@ump.edu.my; Phone:+6095492207; Fax: +6095462244

ABSTRACT

This paper presents the effect of engine speed on the engine performance of 4-cylinder direct injection (DI) hydrogen fueled engine. The 4-cylinder direct injection hydrogen engine model was developed utilizing the GT-Power commercial software. This model employed one dimensional gas dynamics to represent the flow and heat transfer in the components of engine model. Sequential pulse injectors are adopted to inject hydrogen gas fuel within the compression stroke. Injection timing was varied from 110^0 before top dead center (BTDC) until top dead center (TDC) timing. Engine speed was varied from 2000 rpm to 6000 rpm. The validation was performed with the existing previous experimental results. The negative effects of the interaction between ignition timing and injection duration was highlighted and clarified. The acquired results show that the engine speeds are strongly influence on the optimum injection timing and engine performance. It can be seen that the indicated efficiency increases with decreases of engine speed; power increases with the decreases of engine speed; indicated specific fuel consumption (ISFC) increases with increases of engine speed. The injection timing of 60^0 BTDC was the overall optimum injection timing with a compromise.

KEYWORDS: *Direct injection, Injection timing, Engine performance, Engine speed, Hydrogen fuel.*

1. INTRODUCTION

With increasing concern about the energy shortage and environmental protection, research on improving engine fuel economy, hydrogen fueled engine is being developed into a hydrogen fueled engine with manifold injection, direct injection or duel injection according to the fuel supply method [1-3]. Of course, the hydrogen fueled engine with direct injection can fundamentally keep backfires from occurring so it can be utilized as a high powered hydrogen power system if the reliability of high pressure direct injection valve is secured [4]. In today's modern world, where new technologies are introduced every day, transportation's energy use is increasing rapidly. Fossil fuel particularly petroleum fuel is the major contributor to energy production and the primary fuel for transportation. Rapidly depleting reserves of petroleum and decreasing air quality raise questions about the future. As world awareness about environment protection increases so does the search for alternative to petroleum fuels. Hydrogen can be used as a clean alternative to petroleum fuels and its use as a vehicle fuel is promising in the effects to establish environmentally friendly mobility systems. So far, an extensive study investigated hydrogen fueled internal combustion engines (H_2ICE) with external mixture formation fuel delivery system [5-6]. However, the operation of these engines subjected to abnormal combustion, such as pre-ignition, backfire and knocking. Moreover, the power outputs of these hydrogen engines are about 30% less than those of gasoline engines [7]. Therefore the premixed-charge spark ignition engines fueled with hydrogen can be used for significantly limited operation range [8].

Injection timing plays a critical role in the phasing of the combustion, and hence the emissions and torque production. Therefore, extensive number of studies indicated the significance of optimization for ignition timing [9-11]. White et al. [10] suggested that late injection can minimize the residence time that

a combustible mixture is exposed to in-cylinder hot spots and allow for improved mixing of the intake air with the residual gases. This selection can control pre-ignition problem. The main challenge for selecting the proper ignition timing that is in-cylinder injection requires hydrogen–air mixing in a very short time. This study attempts to optimize injection timing that gives the best performance of a 4-cylinders direct injection. The 4-cylinder direct injection hydrogen fueled engine model is developed for this purpose. The effects of engine speed on the injection timing and engine performance such as indicated efficiency, indicated specific fuel consumption, power and torque for direct injection hydrogen fueled engine.

2. MODEL DESCRIPTION

The engine model for an in-line 4-cylinder direct injection engine was developed for this study. Engine specifications for the base engine are tabulated in Table 1. The specific values of input parameters including the AFR, engine speed, and injection timing were defined in the model. The boundary condition of the intake air was defined first in the entrance of the engine. The air enters through a bell-mouth orifice to the pipe. The discharge coefficients of the bell-mouth orifice were set to 1 to ensure the smooth transition as in the real engine. The pipe of bell-mouth orifice with 0.07 m of diameter and 0.1 m of length are used in this model. The pipe connects in the intake to the air cleaner with 0.16 m of diameter and 0.25 m of length was modeled. The air cleaner pipe identical to the bell-mouth orifice connects to the manifold. A log style manifold was developed from a series of pipes and flow-splits. The total volume for each flow-split was 256 cm^3. The flow-splits compose from an intake and two discharges. The intake draws air from the preceding flow-split. The flow-splits are connected with each other via pipes with 0.09 m diameter and 0.92 m length. The junctions between the flow-splits and the intake runners were modeled with bell-mouth orifices. The intake runners for the four cylinders were modeled as four identical pipes with .04 m diameter and 0.1 m length. Finally the intake runners were linked to the intake ports which were modeled as pipes with 0.04 m diameter and 0.08 length. The air mass flow rate in the intake port was used for hydrogen flow rate based on the imposed AFR.

Table 1. Engine specification

Engine Parameter	Value	Unit	Engine Parameter	Value	Unit
Bore	100	mm	Compression ratio	9.5	
Stroke	100	mm	Inlet valve close, IVC	-96	^{0}CA
Connecting rod length	220	mm	Exhaust valve open, EVO	125	^{0}CA
Piston pin offset	1.00	mm	Inlet valve open, IVO	351	^{0}CA
Total displacement	3142	(cm^3)	Exhaust valve close, EVC	398	^{0}CA

In the powertrain, the induced air passes through the intake cam-driven type valves with 45.5 mm of diameter to the cylinders. The valve lash (mechanical clearance between the cam lobe and the valve stem) was set to 0.1 mm. The overall temperature of the head, piston and cylinder for the engine parts are listed in Table 2. The temperature of the piston is higher than the cylinder head and cylinder block wall temperature because this part is not directly cooled by the cooling liquid or oil. The exhaust runners were modeled as rounded pipes with 0.03 m inlet diameter, and 80^0 bending angle for runners 1 and 4; and 40^0 bending angle of runners 2 and 3. Runners 1 and 4, and runners 2 and 3 are connected before enter in a flow-split with 169.646 cm^3 volume. Conservation of momentum is solved in 3-dimentional flow-splits even though the flow in GT-Power is otherwise based on a one-dimensional version of the Navier-Stokes equation. Finally a pipe with 0.06 m diameter and 0.15 m length connects the last flow-split to the environment. Exhaust system walls temperature was calculated using a model embodied in each pipe and flow-split. Table 3 are listed the parameters used in the exhaust environment of the model. Figure 1 shows the entire model of 4-cylinder direct injection engine.

Table 2. Temperature of the mail engine parts

Components	Temperature (K)
Cylinder head	550
Cylinder block wall	450
Piston	590

Table 3. Parameters used in the exhaust environment

Parameters	Value	Unit
External environment temperature	320	K
Heat transfer coefficient	15	W/m^2K
Radiative temperature	320	K
Wall layer material	Steel	
Layer thickness	3	mm
Emissivity	0.8	

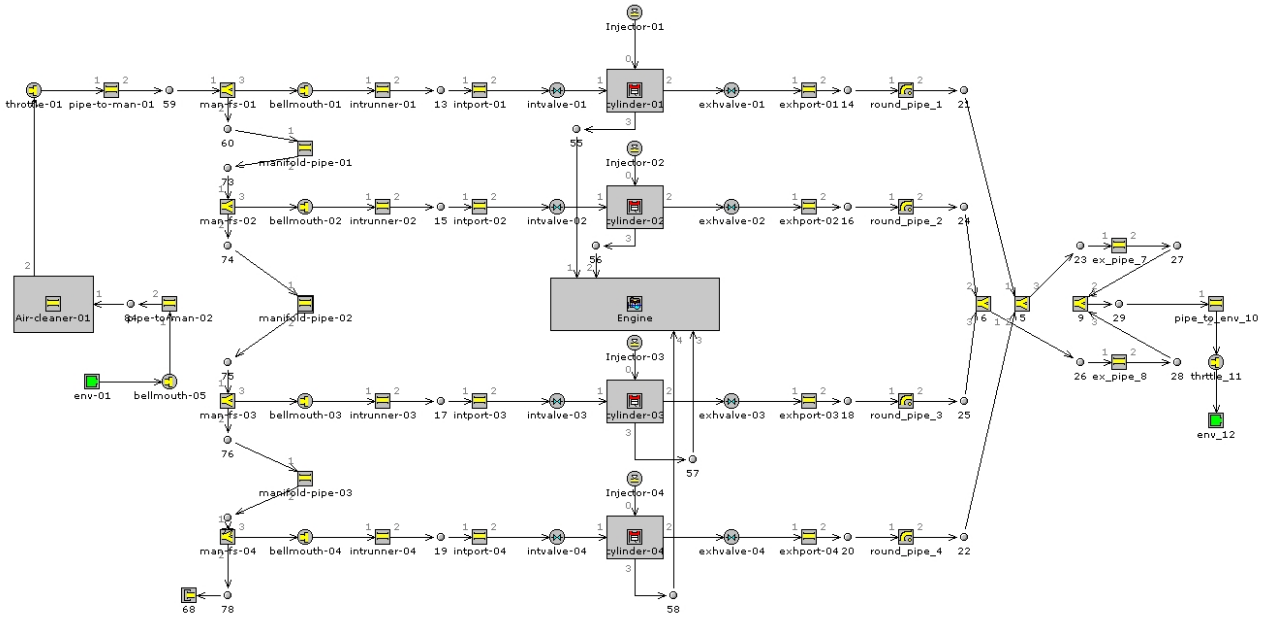

Fig. 1. In-line 4-cylinder direct injection hydrogen fueled engine model

3. RESULTS AND DISCUSSION

The results in the following section show the engine performance behavior with injection timing for each condition under investigation. In order to check the validity and accuracy of the present model, comparison with published experimental results in the literature. The effect of engine speed with injection timing on the engine performance parameters including indicated efficiency, brake specific fuel consumption, power, and torque were discussed. In the present model, hydrogen was injected into the cylinder within a timing range started just before IVC (-96^0 BTDC) until TDC (0^0). Amount of hydrogen injected in one cycle is approximately 22 mg/cycle with injection pulse duration of 4.4 ms. Engine speed was varied from 2000 rpm to 6000 rpm. Stoichiometric condition was fixed throughout the investigation.

The experimental results obtained from Mohammadi et al. [11] were used for the purpose of validation in this study. For the purpose of validation, single cylinder direct injection engine model converted to 4-cylinder direct injection model. The correlation of brake thermal efficiency of the baseline model and experimental results obtained from Mohammadi et al. [11] is shown in Fig. 2. It can be seen that the brake thermal efficiency are good match with the experimental results. Only small deviation was obtained due to the difference between the engine operation conditions that are not mentioned in Mohammadi et al. (2007). However, considerable coincident between the single cylinder model and experimental results can be recognized in spite of the mentioned model differences.

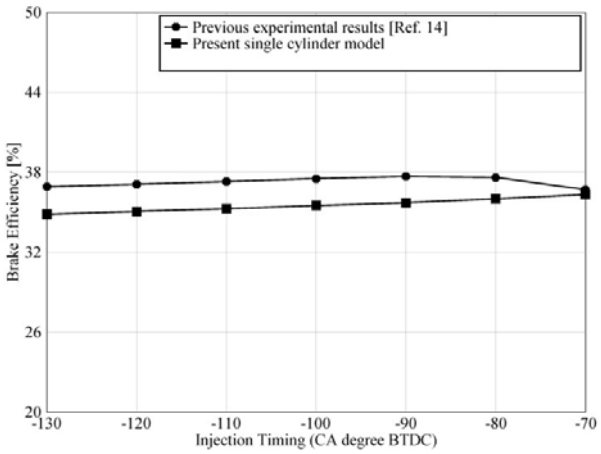

Fig. 2. Comparison between published experimental results [11] and present single cylinder direct injection engine model based on brake efficiency

Figure 3 shows the variation of indicated thermal efficiency with the injection timing for the changes of engine speed. It can be seen that the indicated efficiency increases with decreases of engine speed. From the acquired results, indicated efficiency increases slightly with advances of injection timing towards TDC for all engine speed range. It is also seen that the slightly increase of indicated efficiency until about 30^0 BTDC for 2000 rpm then it drops down. The rate of change in indicated efficiency is higher for higher speed and drop occurs early in higher speeds. For very high speeds, the drop happens earlier due to the early interaction between the injection duration and ignition timing. Optimum injection timing under speeds from 2000 rpm to 5000 rpm was in the range (40°-80°) BTDC while the optimum injection timing for 6000 rpm was 100° BTDC. Obviously, engine speed has a strong contribution in specifying the optimum injection timing. The very limited acceptable injection timing range occurs for high speeds. The selection of the proper injection timing is crucial not only for performance aspects, but also for stable operation. The variation of engine speed on the indicated efficiency is shown in Fig. 4 for stoichiometric operation and injection timing of 100^0 BTDC. It can be seen that the maximum indicated efficiency is 38.55% corresponding to engine speed 2500 rpm. This variation of indicated efficiency is primarily due to the variation of the volumetric efficiency.

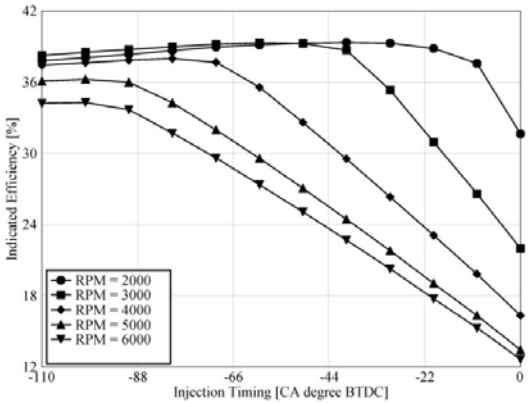

Fig. 3. Variation of indicated efficiency with injection timing for various engine speeds

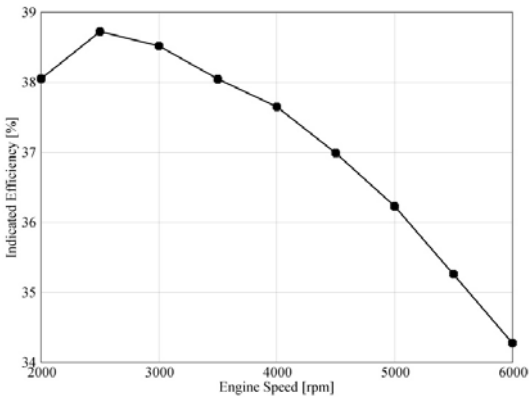

Fig. 4. Effect of engine speed on indicated efficiency

Figure 5 shows the influence of injection timing on ISFC for different engine speeds. Lower engine speeds operation consumes smaller amounts of hydrogen as well as permits wider range for injection timing. The inverse is true for higher speeds where very limited range is available for injection timing. For 2000 rpm, the fuel consumption rates are acceptable throughout the studied range with

injection timing of 60° BTDC being the optimum. At injection timing of 100° BTDC, minimum hydrogen consumed at 6000 rpm. Figure 6 illustrates the variation of power with injection timing with respect to changes the engine speed. It can be seen that the power gained increases with increases of engine speed except 6000 rpm case. However, this happens due to the interaction between injection duration and ignition timing. So, it does not represent the normal situation. This occurs at injection timing in the vicinity of TDC. The maximum power of 123 kW was gained at injection timing of 100° BTDC for 5000 rpm, while the optimum injection timing that gives at 2000 rpm was 40° BTDC and maximum power of 59 kW. The power shows a maximum at engine speed 5000 rpm. It is also observed that the power gained decreases at 6000 rpm due to the increase in the friction losses.

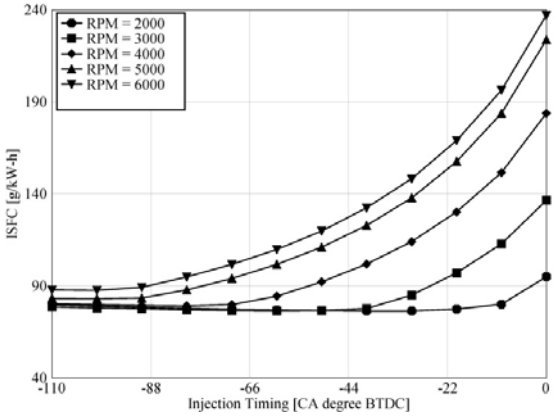

Fig. 5. Variation of ISFC with injection timing for various engine speeds

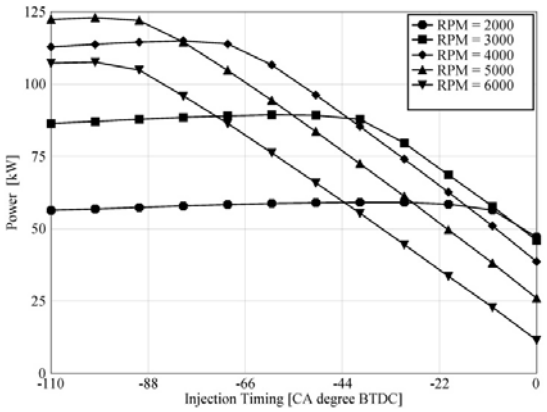

Fig. 6. Variation of power output with injection timing for various engine speeds

The variation of engine speed on the power gained is shown in Fig. 7 for stoichiometric operation and injection timing of 100 ^{0} BTDC. From the acquired results, the power increases slightly with advances of injection timing towards TDC for all engine speed range. It is also seen that the slightly increase of power until about 30^{0} BTDC for 2000 rpm then it drops down. The rate of change in power is higher for higher speed and drop occurs early in higher speeds. For very high speeds, the drop happens earlier due to the early interaction between the injection duration and ignition timing and friction losses. Figure 8 shows the trends of torque with injection timing with the interaction of engine speed effect. Higher torques is produced at lower speed with extra advantages of more acceptable operation range of injection timing. The severe drop with high speed introduces a challenge for injection timing optimization. Based on torque measure, the optimum injection timing throughout the studied speeds, ranged from 40° BTDC at 2000 rpm until 100° BTDC at 6000 rpm. This extended range imposes more control difficulties. However, compromise solutions can be applied.

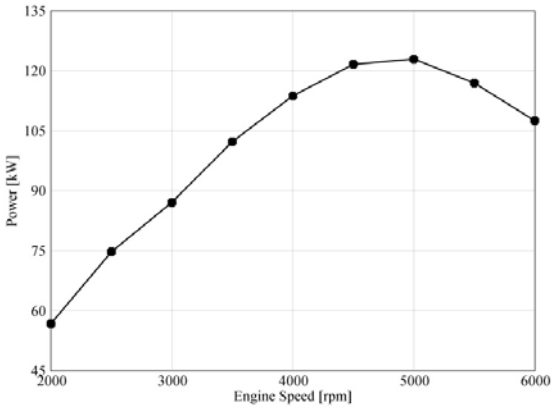

Fig. 7: Effect of engine speed on power

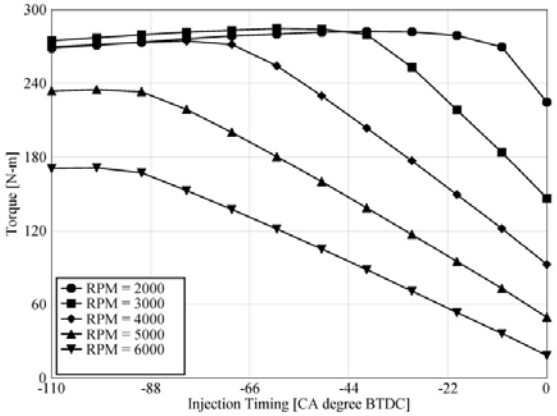

Fig. 8. Variation of torque output with injection timing for various engine speeds

4. CONCLUSIONS

A computational model was developed for four cylinders direct injection hydrogen fueled internal combustion engine. The main results are summarized as follows:

1. The engine performance is strongly depends on the engine speed. The engine speed 2500 rpm gives the maximum indicated efficiency.
2. Optimum injection timing depends also strongly on engine speed. Lower speeds advances optimum injection timing toward TDC timing.
3. As a compromise, injection timing of 60° BTDC can be considered as optimum for the present engine. However, this is for constant injection timing. The recommended operation is with different injection timing bases on engine speed.
4. Interaction between injection duration and spark timing is strongly undesired and can result in unstable operation. This is was apparent by the unaccepted performance parameters during interaction period. Avoidance of this interaction should take priority in specifying injection timing.

5. ACKNOWLEDGMENTS

The authors would like to express their deep gratitude to Universiti Malaysia Pahang (UMP) for provided the laboratory facilities and financial support.

6. REFERENCES

[1] William, F., Stockhausen S. et al., Ford P2000 hydrogen engine design and vehicle development program. *SAE 2002- 01– 0240*.

[2] Eichlseder, H., Wallner, T., Freymann, R. and Ringler, J., The potential of hydrogen internal combustion engines in a future mobility scenario. *SAE 2003- 01–2267*.

[3] Kim, Y.Y., Lee, J.T. and Choi, G.H., An investigation on the cause of cycle variation in direct injection hydrogen fueled engines. *Int. J. Hydrogen Energy*, 30(2005), pp. 69-76.

[4] Lee, J.T., Kim, Y.Y., Lee, C.W. and Caton, J.A., An investigation of a cause of backfire and its control due to crevice volumes in a hydrogen fueled engine, *Trans ASME.,* 123(2001), pp. 204–10.

[5] Stockhausen, W.F., Natkin, R.J., Kabat, D.M., Reams, L., Tang, X., Hashemi, S., Szwabowski, S.J., and Zanardelli, V.P., Ford P2000 Hydrogen Engine Design and Vehicle Development Program, *SAE Paper No.2002-01-0240*.

[6] Kahraman, E., Ozcanlı, C. and Ozerdem, B., An experimental study on performance and emission characteristics of a hydrogen fuelled spark ignition engine. *Int. J. Hydrogen Energy,* 32 (2007), pp. 2066–2072.

[7] Tang, X., Kabat, D.M., Natkin, R.J., Stockhausen, W.F. and Heffel, J., Ford P2000 Hydrogen Engine Dynamometer Development, *SAE Paper No.2002- 01-0242*.

[8] Tsujimura, T., Mikami, A. and Achiha, N. A Study of Direct Injection Diesel Engine Fueled with Hydrogen. *SAE paper No. 2003-01-0761*.

[9] Kim, Y.Y., Lee, J.T. and Caton, J.A., The development of a dual-Injection hydrogen-fueled engine with high power and high efficiency, *Journal of Engineering for Gas Turbines and Power, ASME,* 128(2006), pp. 203-212.

[10] White, C.M., Steeper, R.R. and Lutz, A.E., The hydrogen-fueled internal combustion engine: a technical review, *Int. J. Hydrogen Energy,* 31(2006), pp. 1292–1305.

[11] Mohammadi, A., Shioji, M., Nakai, Y., Ishikura, W. and Tabo, E., Performance and combustion characteristics of a direct injection SI hydrogen engine. *Int. J. Hydrogen Energy*, 32(2006), pp. 296-304.

Proceedings of the 4th BSME-ASME International Conference on Thermal Engineering 27-29 December, 2008, Dhaka, Bangladesh

THE EFFECT OF COMBUSTION AIR DISTRIBUTION ON COMBUSTION CHARACTERISTICS IN REGENERATIVE COMBUSTION SYSTEM

Waseem Amjad[1],Imtiaz Hussain[1] and In-Lim Gweon[1]

[1]Combustion Engineering Lab. Mechanical Department Myong-Ji University South-Korea

Email: shah_waseem@hotmail.com

ABSTRACT

The innovative combustion technique of continuous staged air (COSTAIR) served as a basis for the development of newly developed regenerative burner. Existing regenerative burner in which a ceramic material is used as a heat storage medium in regenerator for raising the temperature of combustion air for better heating potential of flue gases and reduces fuel consumption. Here in this paper a numerical study has done by ANSYS CFX to visualise the effect of introducing staged combustion air (another factor for enhancing efficiency) rather in bulk form in existing regenerative burners to increase the mixing property. It is analysed this way is effective in redusing all above factors along with NOx more betterly. Due to proper mixing temperature distribution is found to be uniform so heat transfer characteristics enhance.

Keywords*: ANSYS-CFX modelling, continuous staged air, regenerative combustion, preheated air*

1. INTRODUCTION

Design of new burners is mostly based on the long-time experience. Moreover, burners are tested at testing facilities before putting into operation. However this approach is limited by economic constraints (costly prototype manufacture and individual test) as well as technical one (parameters of testing facility). Thus new alternatives of partial and/or complete subsitution of physical burner testing are being investigated with support of up-to date computational tools.

Art of computational methods for the fluid flow prediction including chemical reactions and heat transfer make complex burner simulation possible [1]. On the other hand these computational methods are not reliable.Therefore good knowledge of their strengths and weakness is required [2,3].This article reports modelling of an experimental regenerative burner installed with air distributers.The burner has been designed as a low NOx by introducing combustion air staged-wise. The geometry of air- distributers modified with respect to amount of NOx emission.

The new development of regenerative burner with air distribution system shown in Fig.1.Since highly preheated air combustion increases the potential of NOx emission, a new method for reducing NOx emission is required. As shown in the figure, for it, this system has a pair of axial tubes as air distributors. Both of these tubes are placed axially infront of each other. The combustion air flows through the inner annulus of these tubes and then entered through the circuler opening into the furnace. The total amount of combustion air can be contrlled by 4-way valve as in Fig:1.Here the main objective of simulation is to show a

comparative difference between existing one and this new one and then to fix a proper air-distributor with respect to mixing of air with fuel for low NOx and will not cause maximum rise of pressure with in the furnace. This made simplification for modelling that main part of system (furnace,fuel nozzle and air-distributor) is modeled to optimise the air-distributor configuration.

Fig:1 Layout of testing burner and testing air-distributors

A two side arrangement of air distribution along with fuel is shown in Fig.1.The main aim of simulation was to select an optimum air distributor which estimate the minimum pressure development inside furnace along with NOx. Because in this arrangement flue gases will have to pass through these openings (atleast 50% of the incoming air), this can cause a strong turbulence at that side acting as outlet. So that,s why only the furnace having air distributors was modeled as shown in Fig. 2.The new combustion consept in regenerative combustion with continued air staging have been developed and to provide a base for experimental and commersial developments a numerical analysis has done.

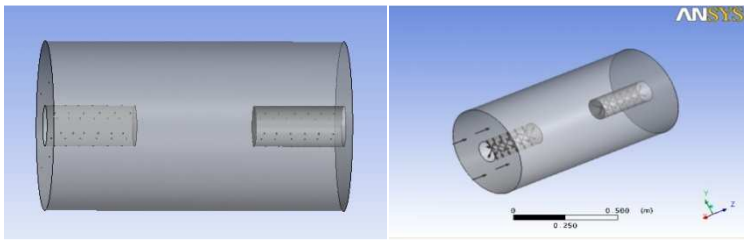

Fig.2 The design model of the COSTAIR burne that consists of a coaxial annulus. The combustion air is distributed into the furnace by means of an air distributor with numerous openings.

2- CONTINUED STAGED AIR COMBUSTION (COSTAIR)

The COSTAIR combustion concept have been developed for application in boilers.The main principle is a continued staging of the combustion air in order to supress the thermal NOx. Its operation is stable and free of pulsation over a wide operating range (air ratio up to 5). NOx emission values are <10 ppm (15%O_2) and CO emission are <5 ppm (5%O_2) under atmospheric conditions [7,8].

3- COMPUTATIONAL MODELLING

Computational model was set up in ANSYS-CFX software. Simplifying assumptions introduced to the model are the following: Firstly, the whole of the set-up was not modelled. This simplification uses an assumption that only the parts which cause air distribution in furnace will have effect on mixing properties and pressure development. Second geometry simplification concerns the inspection holes in the chamber, which were neglected as well as annular volume filled with cooling water. It was modelled as constant temperature wall boundary condition.The surface of computaional mesh is displayed in Fig:3.Tetrahedral mesh element are applied around more complicated features such as fuel nozzles and air openning while hex/ wedge element elsewhere [2,3]. Detail of them in table 1.

Table:1 Mesh Information

Number of nodes	Number of elements	Tetrahedra	Wedges
447089	1961542	1698052	263490
Face angle	Min: 6.21053 [degree]	Max: 89.3385 [degree]	
Length ratio	Min: 1.07111	Max: 17.5155	
Volume ratio	Min: 1.00008	Max: 181.555	

In order to identify optimum arrangement of the air opening in terms of minimum pressure accurance in to the furnace and NOx formation a set of 6 (3 × 2) different arrangment were introduced. Fig. 4 shows the cross-sectional veiw of air-distributor having different positions of air openings.

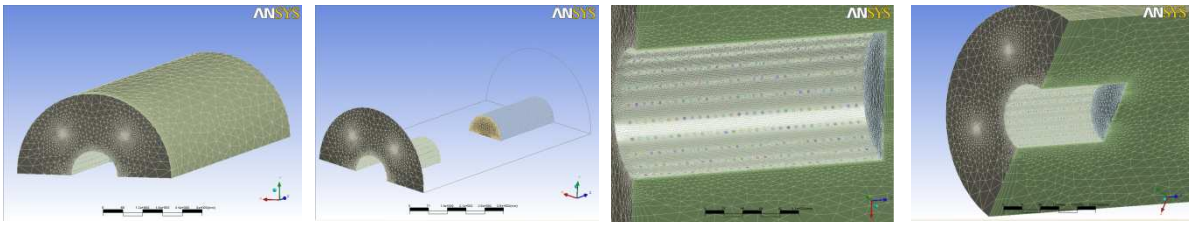

Fig: 3 Computational mesh.

Table:2 Alternatives of air-distributor to be analysed.

Diameter	Degree	Number of openings
2 mm	15	720 (24 × 30)
	30	360 (12 × 30)
3 mm	15	720 (24 × 30)
	30	360 (12 × 30)
4 mm	15	720 (24 × 30)
	30	360 (12 × 30)

Chemical reactions were modelled by the following two step model for methane combustion:

$2CH_4 + 3O_2 \longrightarrow 2CO + 4H_2O$

$2CO + O_2 \longrightarrow 2CO_2$

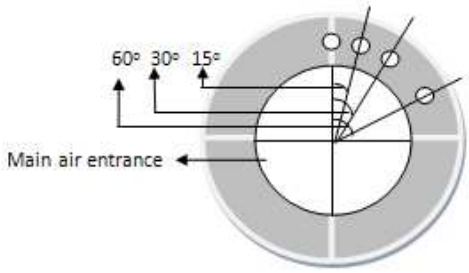

Fig:4 Distribution of air openings of air-distributor.

Rates of chemical reaction were calculated using well-known eddy-dissipation model of Magnussen and Hjertager [7], which relates the rate of reactions to the local turbulence properties (representing intensity of turbulent mixing). This model is best applied as the chemical reaction rate is fast relative to the transport processes in the flow and also that fuel and oxidant be available in the control volume for combustion to occur. There is no kinetic control of the reaction process. Thus, ignition and processes where chemical kinetics may limit reaction rate may be poorly predicted. The specified chemical time scale may need to be adjust in order to achieve best results for specific problem. For methane-air combustion, good starting points are 1.37e-4 [s] when applying Kolmogorov time scale, or 5e-4 [s] when applying to the mixing time scale and this was applied as Kolmogorov time scale tends to be more aggressive and lead to global extinction of flame [2,3].Boundry conditions were set up as follow:

- Velocity inlet for incoming fuel
- Velocity inlet for air openings
- Pressure outlet at the flue gas outlet
- Constant temperature wall for the cooled outer surface of the furnace shell

The compelete set of six alternatives of the different positions of the air openings was calculated. After an acceptable level of convergence computation of NOx formation took place based on the obtained results. As the fact that fuel does not contain any chemically bounded nitrogen, all of the NOx produced is accounted by the two following formation mechanism [8]:

- Thermal (Zeldovich) mechanism and
- Promt mechanism

Due to the turbulence nature of the flames, influence of turbulent temperature fluctuations on formation of NOx also needed to be included. Concentration of H/OH radicals were calculated using assumption of partial chemical equilibrium.

5- ANALYSIS OF RESULTS

Firstly the following figures show a comparative difference of combustion behaviour in conventional and conventional with air distribution. In conventioanl furnace NOx formation is more close to inlets while in air distribution case it is farther along the furnace due to continous combustion as in fig:5. Similarly distribution of oxygen in fig:6 show distribution in both cases.Secondly,in air distribution case, pressure development inside the furnace and NOx outlet concentration were the primary monitored parameters.These parameters are shown in Table 3.It may be observed from the displayed data that the NOx emission differ slightly depending upon air flow rate. On the other hand pressure development differ

significantly depending upon the total cross sectional area for outflow of gases. Smaller way for exit of flue gaes causes the high turbulence viscosity at outlet which leads to high pressure as shown in Fig. 7&8

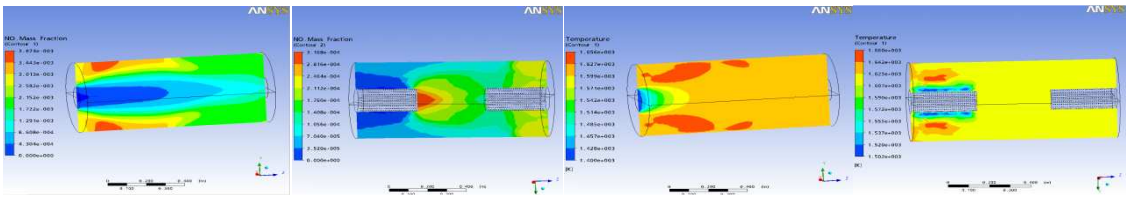

Fig:5 Nox and temperature distribution in conventional and with air distributor furnaces. from left NOx and temperature in both cases respectively.

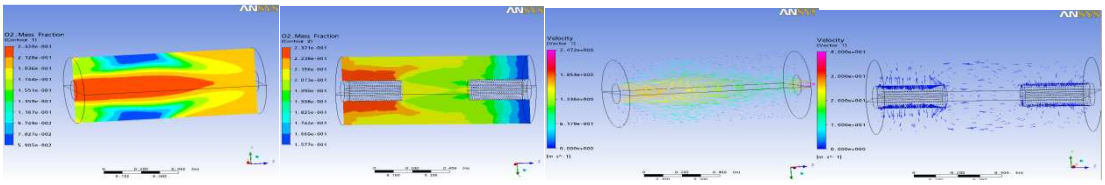

Fig:6 Oxygen and velocity distribution pattern in conventional and with air distributor furnaces.from left oxygen and velocity in both cases respectively.

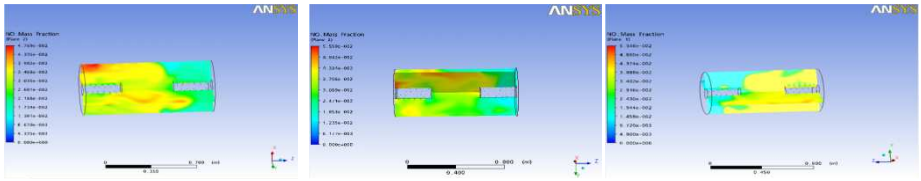

Fig:7 From left NOx distribution with 2,3 and 4mm diameter respectively of air opening distribued at 15^0

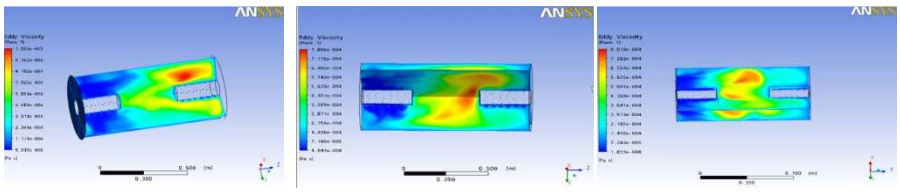

Fig:8 Development of turbulence especially at exit side (causing high pressure) with 2,3 4mm diameter respectively of air opening distribued at 15^0

Table: 3 NOx concentration at outlet and pressure of furnace .

Diameter	Degree	Pressure [Pa]	NOx [ppm]
2 mm	15	118	6.54
	30	170	7.98
3mm	15	110	6.10
	30	133	7.20
4mm	15	80	5.21
	30	102	7.01

CONCLUSION

The article demonstrate one of the possibilities of utilisation of computational tool in terms of finding optimum arrangement of air distributor of an experimental burner. Different alternatives were investigated with respect to NOx production and pressure occurance.It is analysed that application of air distribution in regenerative system provide positive results in sence of temperature and NOx formation. Finally, an alternative corresponding to minimum NOx production and pressure development was identified. However, this represents only a first step for experiment, the next step which is under process is to make a set-up for the validation of these results and to provide a base for commercial level.

FUTURE WORK

This is the first part of our work, the next which is going on is experimental setup for better support in the application of this continous staging air (COSTAIR) technology in regenerative burners.

REFERENCES

Book

[1] Theoretical nad Numerical Combustiion" by Thierry Poinsot, et al

Chapters

[2] ANSYS Release11.0 Documentation for ANSYS Workbench**,** www.kxcad.net/ansys
[3] ANSYS CFX, Release 11.0**,** www.kxcad.net/ansys/index.htm

Conference

[4] Gyung-Min, Advanced low NOx combustion using highly preheated air, Energy conversion and Management 42(2001) 639-652
[5] D. Veynante, Turbulent combustion modeling, Prog. Energ. Comust. 28 (2002) 193-266

Report

[6] A.H. Lefebvre, Gas Turbine Combustion, Taylor & Fracis, 1998, ISBN 1-56032-673-5.
[7] A. Al-Halbouni, The COSTAIR Gas burner: extremely low NOx and CO emission, joint British-French Days, Guernsey, Channel Islands, 1998.

Conference

[8] R. Giese, A. Al-Halbouni, R. Sontag, The influence of air and fuel impulses on the emission behaviour of the COSTAIR Gas burner, in 5th European Conference on industral furnaces and boilers, Portugal 2000

Proceedings of the 4th BSME-ASME International Conference on Thermal Engineering
27-29 December, 2008, Dhaka, Bangladesh

COMPARISON OF THE PERFORMANCE AND EMISSIONS OF A PETROL ENGINE USING A RANGE OF UNLEADED FUELS

S. A. Breffit, M.G. Rasul and A. A. Chowdhury

College of Engineering and Built Environment
Faculty of Sciences, Engineering and Health
Central Queensland University, Rockhampton, QLD 4702, AUSTRALIA

E-mail: m.rasul@cqu.edu.au

ABSTRACT

The use of fossil fuels for transportation purposes has increased significantly over the last 60 years, and the environmental effects of the use of fossil fuels have become a matter of concern in recent years. This has lead to the development of a number of fuels which are intended to reduce the environmental impact of the ever-growing use of motor vehicles. There are a number of views on the advantages and disadvantages of these fuels, such as dispute as to the life-cycle emissions and the impact on performance. It is the aim of this paper to present independent findings into the performance and emissions pros and cons for some alternative fuels, Regular Unleaded (91 octane), Premium Unleaded (95 octane) and Premium Unleaded, Ultimate (98 octane). In a full scale laboratory testing undertaken at Central Queensland University, it is found that Premium Unleaded and the Ultimate offer better power and torque efficiency with a grater percentage of specific fuel consumption compared to regular unleaded petrol. Moreover, the Ultimate appeared to have less exhaust emissions with lower concentration of all pollutants compared to regular unleaded petrol.

Keywords: *Unleaded Fuels, Petrol Engine, Emissions.*

1. INTRODUCTION

The term, greenhouse gas, refers to those gases which are believed to contribute to global warming through the greenhouse effect. This is due to the ability of these gases to absorb infrared radiation from the sun. Whilst they are all naturally occurring gases, the levels of a number of these gases in the atmosphere as a result of human activity are of concern within the global community. In recent years a great deal of concern has been raised regarding the apparent increase in global temperature, which is believed to be the result of an increase in the atmospheric concentration of a number of gases. These gases, termed greenhouse gases for the heating effect that they have on the Earth, include water vapour (H_2O), carbon dioxide (CO_2), methane (CH_4) and nitrous oxide (N_2O). Water vapour, carbon dioxide and methane are products of the combustion process used in internal combustion engines. Water vapour causes the largest impact on global warming (between 36% and 66%) out of all of the greenhouse gases, however the concentration of water vapour in the atmosphere is not directly affected by human activity as it has a short lifespan in the atmosphere [1]. When addressing the issue of climate change and greenhouse gases, it is

important to consider the impacts of human activity (anthropogenic impacts), as changes in human activity affect the levels of certain greenhouse gases. Carbon dioxide is the most prevalent of these greenhouse gases, making up approximately 72% of the total anthropogenic greenhouse gas emissions [2]. This equals approximately 25,028 million metric tonnes of carbon dioxide being released into the atmosphere each year, based on 2003 figures. Carbon dioxide emissions are responsible for between 9% and 26% of the total global warming impact [1]. Transportation emissions account for 14% of all greenhouse gas emissions, and 19.2% of carbon dioxide emissions [3]. This is a significant portion, and it has been suggested that by using alternative transport options, there will be a significant saving of greenhouse gas emissions.

There are a number of "alternative fuels" which are believed to be more environmentally friendly than fossil fuels. Some of these fuels are made from plant matter, which has the advantage of absorbing carbon dioxide while growing. One of these fuels is ethanol, whose use in the transportation sector is due to its ability to be mixed with standard petroleum based fuels such as petrol and gasoline, which reduces dependence on fossil fuels. As ethanol comes from a renewable source such as plant matter, emissions from its combustion are not considered to contribute to raising carbon dioxide stocks in the environment [4]. The burning of fossil fuels for transportation makes up approximately 14% of the global greenhouse gas emissions each year. In response to this, a number of options have been investigated as possible ways of reducing this impact on the environment. Such possibilities include electric vehicles, hydrogen fuelled vehicles, hybrid petrol/electric vehicles and fuels which are designed to produce less greenhouse gas emissions than regular fossil fuels. Petroleum products such as Premium Unleaded and unleaded petrol containing small amounts of ethanol are two examples of these claimed 'emission reducing' fuels. In Australia, the options for unleaded fuels include Unleaded (91 octane), Premium Unleaded (95 octane), a higher grade of premium unleaded (e.g. Ultimate from BP, 98 octane) and a mix of regular Unleaded petrol containing up to 10% ethanol which is commonly referred to as e10.

Bouris *et al.* [5] summarized the growing importance of understanding and controlling particulate emissions from gasoline engines and an experimental simulation approach was described with the potential for exploring particle deposition/capture and oxidation phenomena under well-controlled conditions. It was done by using artificially generated sub-100 nm carbon particles into a synthetic exhaust gas stream and by simulating engine-out soot emissions. Ochieng *et al.* [6] explained a vehicle performance and emission monitoring system and referred the procedures used to validate the data generated by both diesel and petrol powered vehicles. The system attains the specified performance levels for each of the subsystems, with aggregate mass emissions within 11.5%, 8.1% and 17.7% for CO, CO_2 and NO, respectively. Arapatsakos *et al.* [7] discussed the use of the fuels propane and butane-propane (80:20) in a four-stroke engine made to function with gasoline (petrol). It was observed that gas emissions were reduced compared with gasoline and the reduction for carbon monoxide emissions was found greater when butane-propane was used. Ristovski *et al.* [8] conducted a comparative study of the particle and carbon dioxide emissions from a fleet of six dedicated liquefied petroleum gas powered and five unleaded petrol powered new Ford Falcon Forte passenger vehicles at four different vehicle speeds—0 km/h, 40 km/h, 60 km/h, 80 km/h and 100 km/h. The study reported that the particle number emission factors ranged from 1011 to 1013 per km and was over 70% less with liquefied petroleum gas compared to unleaded petrol. Sayin *et al.* [9] studied the effect of using higher-octane gasoline (petrol) than that of engine requirement on the performance and exhaust emissions and showed that higher octane ratings than the requirement of an engine not only decreases

engine performance but also increases exhaust emissions. Exhaust emissions from vehicles consist of a hot and complex mix of both gaseous CO_2) and particle phases range in size from 10 to 80 nm [9]. This study presents an experimental study to determine emissions and fuel consumption rates of petrol driven cars with some alternative unleaded fuels, Unleaded (91 octane), Premium Unleaded (95 octane) and Premium Unleaded, Ultimate (98 octane) available in Australian market.

2. METHODOLOGY

In order to understand the real world effects of using alternative fuels, several laboratory tests were conducted. By running an engine in the same situations using different fuels, it was anticipated that the differences between the fuels would be apparent. The test procedure was developed to enable the engine and exhaust characteristics to be investigated at a number of different engine speeds and air-fuel ratios. This procedure was developed specifically to suit the equipment available and the aims of this study.

2.1 Equipment

All of the equipment and software involved in the testing and data acquisition was supplied to Central Queensland University by Dyno Dynamics. The engine used in this study is a 2.4 litre four cylinder Toyota petrol engine (model 2AZ-FE) which is commonly found in modern Camry and Rav4 vehicles. The engine is in very good condition, having only been used occasionally for laboratory experiments and demonstrations. The dynamometer used is an engine type dynamometer, as opposed to the more commonly used chassis dynamometer. Its primary component is an electromagnet which applies a braking force to the engine drive shaft. This serves two purposes – to enable the calculation of the power and torque generated, and to control the engine speed as required by the test procedure.

The gas analyser used to analyse the exhaust gases is an Andros Model 6241A, and is capable of non-dispersive infrared as well as electrochemical analysis. This allows for the measurement of hydrocarbons (n-Hexane), carbon monoxide (CO), carbon dioxide (CO_2), oxygen (O_2) and NO_x (Nitric Oxide and Nitrogen Dioxide). It is important to note that the gas analyser detects a wide range of hydrocarbons, via a non-dispersive infrared sensor, and not just n-Hexane. While it is most effective at detecting n-Hexane due to its setup, it is compensated to give a good indication of the levels of other hydrocarbons.

2.2 Laboratory Process

The procedure was developed to test the performance and emissions of the engine at seven different speeds – 1200rpm, 1800rpm, 2400rpm, 3000rpm, 3600rpm, 4200rpm and 4800rpm. Each test run consisted of running the engine at a specified speed for 2 minutes to obtain stability in the performance and emission readings, and then recording the data 10 times within 20 seconds. The engine speed was then changed and the system allowed to stabilise and the test was repeated. This process was repeated until each of the 7 engine speeds has been tested 5 times. In order to minimize the effects of atmospheric variation throughout the testing, all experimental work was completed between the hours of 11am and 5pm. Testing was avoided on rainy days, and when the atmospheric conditions were considerably different from other test days.

2.3 Analysis Details

The data obtained was graphed with each characteristic plotted against the engine speed, or against air-fuel ratio or exhaust gas temperature where relevant. The graphical results clearly show the advantages and disadvantages of each fuel. For a large enough samples from a population, according to the Central Limit Theorem, the distribution of the sample mean is approximately normal, no matter what population it was drawn from [10]. The size of the sample required for this approximation to be valid is specified as greater than 30. As the test procedure in this study requires 50 samples of data to be taken for each point, it is possible to use this theorem. The Central Limit Theorem is important in analysing the results of this study, particularly the graphs produced. Since the sample of data taken approximately forms a normal distribution, 95.45% of sample values will lie within two standard deviations of the mean.

The Wilcoxon Rank-Sum Test is a statistical process that is used to determine whether two population means are statistically different. This is of importance in this study as the data is obtained from a laboratory situation with a number of inherent inaccuracies. The result of these inaccuracies is that some of the observed differences between the fuels are actually from experimental variation rather than the use of different fuels.

3. EXPERIMENTAL RESULTS AND DISCUSSIONS

The comparison of power, torque and specific fuel consumptions are shown in Figures 1, 2, and 3 respectively. Each graph shows a comparison of the characteristics of the three fuels. It must be noted that the data used for Ultimate is based on 20 measurements, instead of 50 measurements as with the other fuels. This is due to complications with the throttle, and as a result, the variance of these values may be higher.

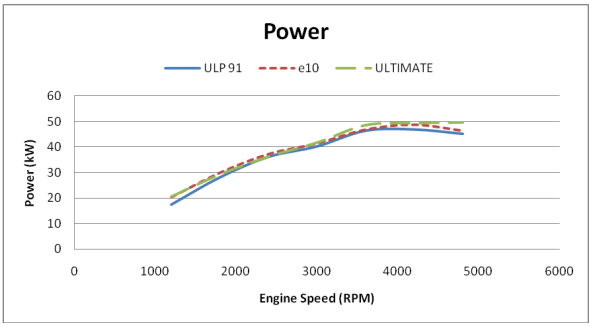

Figure 1: Comparison of engine brake power

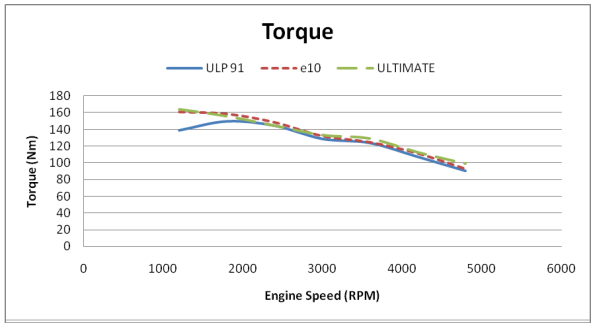

Figure 2: Comparison of engine brake torque

As shown in Figure 1, the power produced by the engine using each of the different fuels differed slightly. It appears at first glance that Ultimate produced slightly more power than the other fuels, however the complications experienced with the throttle during testing for Ultimate must be taken into consideration. The results of this study put the power of the engine approximately 5.07% higher than regular unleaded when using e10, and 6.7% higher than regular unleaded when the Ultimate is used. The peak power produced was 47kW, 48.9kW and 49.8kW for regular unleaded, e10 and Ultimate respectively. It was expected that the Ultimate would produce a higher power output, as its net calorific value is approximately 2.3% (by volume) higher than that of regular unleaded. The e10 fuel was expected to produce less power than regular unleaded fuel, due to its lower net calorific value. The 5.07% increase

in power can possibly be explained by the extra oxygen content in the ethanol blend fuel causing the fuel to combust more completely. This explanation is supported by the fact that the carbon monoxide emissions are lower, and carbon dioxide emissions are higher when using e10. In Figure 2, the torque measurements vary with each different fuel by the same percentage as with the power measurements. This is expected as power is a function of torque. The maximum torque produced for regular unleaded was 149Nm, 161Nm for e10 and 164Nm for Ultimate. The specific fuel consumption (Figure 3) shows that per kilowatt-hour of energy produced, both e10 and Ultimate use less fuel (approximately 2.7% less for e10, and 1.6% less for Ultimate, on a mass basis) than regular unleaded.

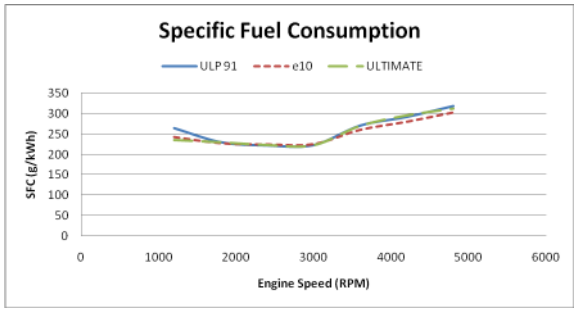

Figure 3: Comparison of the specific fuel consumption

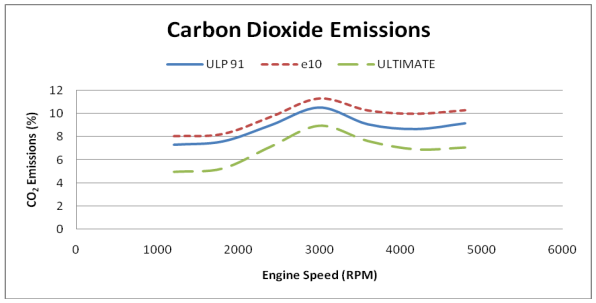

Figure 4: Comparison of carbon dioxide emissions

The analysis of combustion products (Figures 4-8) is quite difficult, as there are a number of variables which are interlinked. It is important to take a holistic approach to determining the causes of the changes in emissions, as one explanation may be contradicted by one or two of the other emissions. While the engine was running on e10, generally the carbon dioxide emissions were about 10% higher, carbon monoxide and hydrocarbons were lower, and the NO_x emissions were higher, compared with the engine running on regular unleaded. The increase in carbon dioxide coupled with the decrease in carbon monoxide emissions is a good indicator that the combustion process is good and close to completes. This is also backed up by the fact that hydrocarbons are also lower. Low levels of hydrocarbons in the exhaust gas are an indicator that almost all of the fuel is being burnt completely. The higher oxygen content of ethanol blended petrol is one possible explanation for the more complete combustion that appears to be occurring with e10.

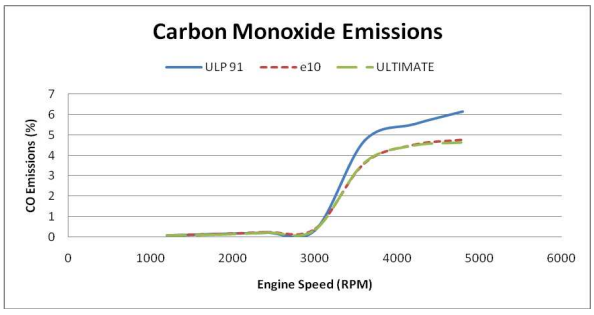

Figure 5: Comparison of carbon monoxide emissions

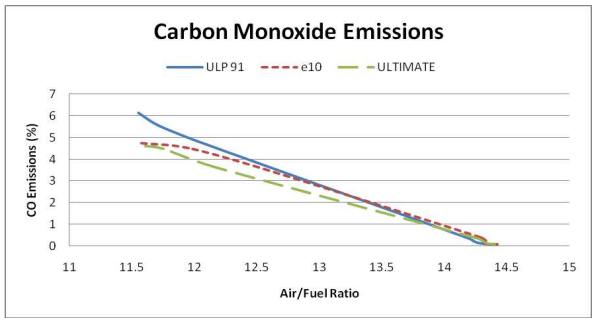

Figure 6:Comparison of carbon monoxide emissions plotted against air-fuel ratio

At higher engine speeds (above approximately 3000rpm), the air/fuel ratio becomes richer and both the carbon monoxide and hydrocarbon emissions increase dramatically

(Figures 4 and 5). This is expected at richer air/fuel ratios as there is insufficient oxygen to burn the fuel completely, and a trend that is common in the results of all of the fuels tested. The exhaust composition when combusting Ultimate unleaded is different from that of both e10 and regular unleaded fuel. There appeared to be quite a large reduction in carbon dioxide in the exhaust – down approximately 22% on regular unleaded. As well as this, the carbon monoxide emissions were also lower, and the concentration of oxygen in the exhaust gas was significantly higher. This was somewhat unexpected, as generally a reduction in carbon monoxide is closely tied with an increase in carbon dioxide. The high level of oxygen in the exhaust indicates that the air/fuel ratio is lean, i.e. there is more oxygen than is required for complete combustion to occur. This supports the fact that there are lower CO emissions, but would suggest that the CO_2 emissions should be somewhat higher (Figure 6).

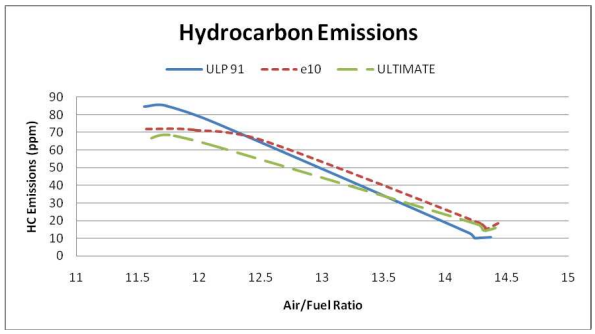

Figure 7: Comparison of hydrocarbon emissions plotted against air-fuel ratio

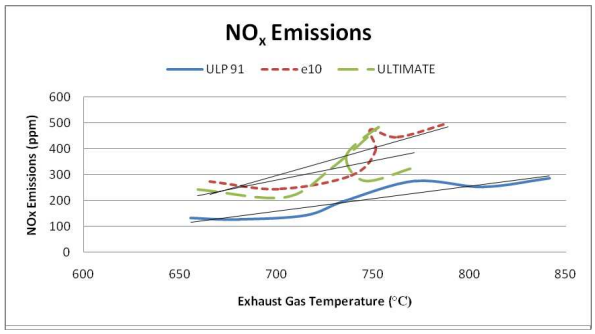

Figure 8: Comparison of NO_x emissions plotted against exhaust gas temperature

As shown in Figure 4, the CO_2 emissions are consistently well below what they are for regular unleaded and e10 indicates that Ultimate is more environmentally friendly. The lower CO and CO_2 emissions are claimed by BP to occur with the use of Ultimate. In Figure 7, the concentration of hydrocarbons is slightly down particularly at higher engine speeds. It is expected that if the combustion is almost complete, that the hydrocarbon concentration would be lower, as there is less unburnt fuel in the exhaust gas, however it must also be considered that the Ultimate has a lower Hydrogen content in the fuel than either of the other two fuels tested. As shown in Figure 8, the NO_x emissions were higher for both e10 and Ultimate than for regular unleaded. This is likely due to poor spark timing caused by the engine's knock sensor struggling to adjust to the new fuel. It is possible that if the engine was run on the new fuels for a longer period of time that the spark timing would be improved and the NO_x emissions would be reduced.

4. STATISTICAL ANALYSIS

The Wilcoxon Rank-Sum Test [11] was used to determine the statistical significance of the results. This is one way to test whether the differences in the results are explainable by variance, or whether the use of a different fuel caused significant changes. In order for this test to show statistical significance, the W values obtained must be either less than 40 (showing that the alternative fuels results are lower than the unleaded results) or greater than 65 (showing that the alternative fuels results are higher than the unleaded results). The W values obtained are shown in Table 1.

Table 1: W- value results of Wilcoxon Rank-Sum test

	Power	Torque	HC	CO	CO_2	NO_x	SFC
e10	56	58	56	51	63	72	51
Ult.	59	59	56	47	33	70	54

It is apparent that when using the Wilcoxon Rank-Sum Test as a comparison method, that the majority of the differences of results obtained are deemed to be statistically insignificant. This is partially due to the fact that this statistical test is considered quite robust, so if something is deemed significant, it is a strong result. The NO_x emissions for both Ultimate and e10 are significantly higher than for regular unleaded, and the carbon dioxide emissions for Ultimate are significantly lower than for regular unleaded. The rest of the results fall in between the values that would make them statistically significant. This does not suggest that using alternative fuels had no impact on these results, but that further testing is required to prove the existence of a relationship between the fuel and the performance and emissions.

5. CONCLUSION AND RECOMMENDATION

This study has investigated the effects on emissions and performance of a petrol engine from the use of a number of 'alternative' fuels. The primary reason for this study being undertaken was to determine the increase or reduction of greenhouse gases emitted, however the results obtained are based on a broader scope. The merits of using ethanol blended fuel and premium fuels were investigated, and for the most part, both fuels presented an improvement in performance and emissions over regular unleaded. As discussed above, users of the e10 fuel could expect approximately 5% improvement in power and torque, while users of Ultimate could expect approximately 6.5% improvement in these areas, compared to the use of regular unleaded petrol. The specific fuel consumption (grams of fuel consumed per kilowatt-hour of energy produced) is approximately 2.7% lower for e10 and 1.6% lower for Ultimate than was recorded for regular unleaded. This indicates an improvement in the fuel consumption, considering the power produced by the engine.

As far as exhaust emissions go, the results were less clearly defined. The e10 fuel had an 11% increase in carbon dioxide emissions and considerably higher NO_x emissions than regular unleaded, whilst the other pollutants were reduced. Ultimate appeared to be a better option in this regard, as its exhaust emissions had lower concentrations of all pollutants except for NO_x, which was in higher concentrations than in the exhaust of regular unleaded, but lower than in the exhaust of e10. Based on the results of this study, it appears that Ultimate is the best fuel of those tested, both in terms of performance and exhaust emissions. The results of this study are, however, not conclusive, and the apparent improvements obtained by using alternative fuels should serve as justification for further testing to be carried out, in order to either verify or refute these findings. It is recommended that further testing be carried out, using both the test procedure used in this study, as well as the test procedure specified in the International Standards, and that a more reliable set of equipment be used to provide more robust results.

REFERENCES

[1] Real Climate 2005, *Water vapour: feedback or forcing?* Retrieved September 12, 2007, from http://www.realclimate.org/index.php?p=142

[2] Rohde, R n.d., *Global Warming Art*, Retrieved September 10, 2007 from http://www.globalwarmingart.com/wiki/Image:Greenhouse_Gas_by_Sector.png

[3] Beer, T, Grant, T, Olaru, D, Watson, H 2004, *Life-Cycle Emissions Analysis of Fuels for Light Vehicles*. Retrieved August 13, 2007, from http://www.greenhouse.gov.au/transport/publications/pubs/lightvehicles.pdf

[4] Costs and Benefits of Mandatory Biofuel Blends in Transport Fuels 2004. Retrieved September 12, 2007, from http://www.med.govt.nz/templates/MultipageDocumentPage____8060.aspx

[5] Bouris, D., Crane, R., Evans, J., & Tippayawong, N. An Approach to Characterization and After-Treatment of Particulate Emissions from Gasoline Engines. *International Journal of Engine Research , 1* (4), 291-300, 2000.

[6] Ochieng, W. Y., North, R. J., Quddus, M., Noland, R. B., & Polak, J. W. Integrated vehicle performance and emission monitoring system. *Transactions of Nanjing University of Aeronautics and Astronautics , 22* (2), 85-90, 2005.

[7] Arapatsakos, C. I., Karkanis, N. A., & Sparis, P. D. Environmental pollution from the use of alternative fuels in a four-stroke engine. *International Journal of Environment and Pollution , 21* (6), 593-602, 2004.

[8] Ristovski, Z. D., Jayaratne, E. R., Morawska, L., Ayoko, G. A., & Lim, M.. Particle and carbon dioxide emissions from passenger vehicles operating on unleaded petrol and LPG fuel. *Science of the Total Environment , 345*, 93 – 98, 2005

[9] Sayin, C., Kilicaslan, I., Canakci, M., & Ozsezen, N. An experimental study of the effect of octane number higher than engine requirement on the engine performance and emissions. *Applied Thermal Engineering , 25*, 1315 – 1324, 2005.

[10] Hollander, M., & Wolfe, D. A. *Nonparametric Statistical Methods* . New York: John Wiley, 1999.

[11] Navidi, W. *Statistics for Engineers and Scientist* .M.A: McGraw-Hill, 2006.

Proceedings of the 4th BSME-ASME International Conference on Thermal Engineering
27-29 December, 2008, Dhaka, Bangladesh

A STUDY OF THE EMISSIONS FROM A DUAL FUEL ENGINE

Nirendra N. Mustafi[1] and Robert R. Raine[2]

[1] Department of Mechanical Engineering,
Rajshahi University of Engineering and Technology, Rajshahi-6204, Bangladesh,
E-mail: nnmustafi@gmail.com
[2] Department of Mechanical Engineering, The University of Auckland, Auckland, New Zealand

ABSTRACT

Biogas is an alternative gaseous fuel that has potentials to be used in dual fuel engines. Although the research works are available on combustion and performance of dual fuel engines using natural gas and methane in literature, published research works on biogas-diesel dual fuel engines are found to be inadequate. Especially the emissions aspects are not well published. The present study is intended to fill the gap and the regulated emissions (such as NO_x, UHC) including particulate matter (PM) are measured for a direct injection diesel engine. Simulated biogas fuels are used in this study. PM is measured by the conventional gravimetric method and PM physical structures are observed visually and are analyzed by scanning electron microscopy (SEM) and transmission electron microscopy (TEM). Results are compared between the diesel and dual fuel operations for the engine operating conditions considered in this study.

Key words: *Biogas, Dual fuel engine, Diesel engine, Emissions, Particulate matter.*

1. INTRODUCTION AND BACKGROUND

Interests have been grown in recent times, in the development of alternative fuels for internal combustion engines, due to the increasing demands for fossil fuels and the associated environmental pollutions. Biofuels (both liquid and gaseous) have shown potentials to be applied in such applications. Biogas can be produced by the anaerobic fermentation of organic wastes. Methane (CH_4) is the main component of biogas, which has a high octane rating and is thus suitable for diesel engines. It has greater potentials to be utilized as an alternative fuel for diesel engines especially in developing nations where there are plenty of resources from which biogas can be generated. The use of biogas also prevents the emission of unused green house gas, CH_4, into the atmosphere. Although diesel engines are efficient, reliable and durable, they produce harmful pollutants such as NO_x and particulate matter (PM). PM emissions from diesel engines are considered as a major source of fine and ultra-fine particles present in the atmosphere [1]. Gaseous fuels mix uniformly with air, resulting in efficient combustion and may cause a substantial reduction in exhaust emissions [2].

Biogas is mainly composed of CH_4 and CO_2 along with trace amount of other hydrocarbons and non-fuel gases. Due to the presence of diluents in biogas it has lower energy content compared to natural gas (NG). CO_2 affects the mixture stoichiometry and the energy input into the cylinder per cycle. It also affects the flame propagation and ignition delay periods. All of these have significant effects on exhaust emissions [3]. Biogas in diesel engines operates in the dual fuel mode, where biogas acts as the primary and diesel acts as the pilot fuel. Gas is normally inducted into the engine along with air and compressed as usual. The pilot diesel (equivalent to 5% to 10% of the total full load fuel flow), is injected through the conventional fuel injection system near the end of the compression stroke to initiate combustion. The pilot diesel first self ignites and then acts as an ignition source for the surrounding gas-air mixture. Dual fuel engines have the flexibility to be operated in either diesel or dual fuel mode and the change over can be done even under load without any interruption to the engine operation. This is quite important where the supply of gaseous fuel may not be reliable.

Numerous works have been published over the last decades on the use of NG in dual fuel engines since Karim [4] to Papagiannakis and Hountalas [2] and Selim [5]. These experimental and computational analyses are directed to have better understanding of the combustion phenomena and engine performance with the consideration of operating parameters. Published research works are also available from emissions perspective for NG-diesel dual fuel engines such as [2,6-8]. However, a very limited number of published research works are found for biogas-diesel dual fuel engines especially on exhaust emissions. Karim and Weirzba [3] and Karim and Amoozegar [9] investigated the effects of CO_2 addition into CH_4 fueling in a diesel engine and reported that up to 25% CO_2 in biogas did not have any significant effect on unburned CH_4 concentration in the exhaust compared to only CH_4 fueling. However, increasing further CO_2 in the fuel resulted in sharp increase in unburned CH_4 concentration in the exhaust. Both the presence and increase in CO_2 content in biogas are reported to reduce the NO_x concentrations in the exhaust rapidly. Virtually no published research work is found dealing the PM emissions from a biogas-diesel dual fuel engine.

The present study investigates the exhaust emissions (NO_x and unburned hydrocarbon (UHC)) with a priority on PM emissions from a biogas-diesel dual fuel engine compared with diesel fueling. Measurements of PM mass concentrations as well as their physical characterization are performed by using SEM and TEM.

2. EXPERIMENTAL PROCEDURE

2.1. Test Facility

A Lister Petter PHW1, direct injection (DI), diesel engine is used for the present study. The major engine specifications are given in Table 1. The original injection system for the diesel fuel is maintained for the dual fuel operation. For dual fuel operation, the gaseous fuel is supplied in the air inlet pipe about half a meter ahead of the inlet valve for mixing with the incoming air and is controlled by a needle valve. Air mass flow rate is obtained by using a Meriam® laminar flow element (LFE); Model: 50MC2-2F. The mass flow rate of gaseous fuel is measured by a Micro®-Motion mass flow meter (Model: D6) which operates on the Coriolis effect vibrating u-tube principle. Diesel flow rate is measured by a volumetric flow measurement system. The output signals from Micro®-Motion and the Meriam® go to a low speed data acquisition system connected to a PC where they are in turn converted into the corresponding mass flow rates.

Simulated biogas is prepared in the laboratory by mixing pipeline NG with CO_2 from a high-pressure cylinder. The simulated biogases are biogas-1 (80% CH_4 and 20% CO_2); biogas-2 (67% CH_4 and 33% CO_2) and biogas-3 (58% CH_4 and 42% CO_2). NO_x emissions are measured using a chemiluminescent analyzer and UHC emissions are measured with flame ionization detector. These equipments are connected with the thermostatically controlled heated sample line, which is maintained at 190°C (see Fig.A2).

Tests are performed at a constant speed of 1750 rpm and with a constant injection timing of 28° before top dead center (bTDC). At first the engine is run with diesel only and then subsequently run with biogases in dual fuel mode. Two modes of steady state operation are chosen for diesel operation: light load (~ 3 Nm) and high load (~ 28 Nm), which are about 8% and 75% of the rated output of the engine respectively for the mentioned speed. Under dual fuel operation, the amount of pilot diesel is kept

Table 1. Engine specifications

Engine type	Lister Petter single- cylinder, DI, water cooled
Bore/Stroke	87.3/110 (mm)
Swept volume	659 (cm^3)
Connecting rod length	231.9 (mm)
Compression ratio	16.5
Injection timing by spill	28°bTDC

minimum (corresponding to 3 Nm load) and constant and increasing biogas flow rate to the engine increases the torque output of the engine to 28 Nm. To ensure consistency in engine operations, the engine is first run at diesel light load with 1750 rpm until the exhaust temperature is stable at around 200°C. Then the measurements are recorded for this condition, which is repeated each day as engine warm-up run. The engine is then run at the desired conditions and is allowed to settle there before recording any measurement. About 62% diesel is replaced during dual fuel operations.

2.2. PM Measurements (Gravimetric Analysis)

A single stage partial flow dilution (PFD) system where a fraction of the total exhaust is sampled is used in this study. The system includes two major parts: a partial flow dilution tunnel (PFDT) and a flow control trolley. Exhaust sample is diluted inside the tunnel and the flow control trolley controls and measures the different mass flow rates involved in the system. At the end of the tunnel there are two filter housings (main and backup filters) where PM filters are located. The pump trolley consists of two rotary vane air pumps and two corresponding mass flow controllers (Sierra Mass Flow Controllers, Model No. 840H-4-OV1-SV1-D-V1-S1). The flow control trolley is manipulated by a data logger (21x Micrologger; Campbell Scientific Inc.), from which the outputs are sent to a PC for recording and further processing. The diluted sample flow rate through the tunnel is maintained at 140 l/min and the dilution ratio is maintained at about 10 to 1 for the whole experiment. The sample transfer tube is insulated and heated maintaining a wall temperature of 190°C to minimize the thermophoretic deposition particle loss [10].

PM samples are collected on PallFlex Fiberfilm T60A20, 70 mm diameter filters. The filter face temperature is maintained at below 52°C [11] during this sampling (about 30°C). Filters are conditioned in an incubator at 22±1°C and 45±2% RH for 18-20 hours before and after use. The filter weighing equipment is a Mettler Toledo MT5 Digital Microbalance, which has a readability of 1μg.

2.3. PM Shape Analysis (SEM and TEM method)

PM samples are collected on 70 mm Isopore™ polycarbonate membrane filters, suitable for SEM [10], with 0.4 μm pore size. Samples are collected for SEM analyses by using the same PFD system. Samples are cut from the filters (approx. 5mmx5mm) and coated with a thin layer (a few nanometers) of platinum to make the samples conductive and suitable for electron microscopy [12]. The coated samples are then analyzed by using a Phillips XL-30S Field Emission Gun (Phillips Electron Optics, NL) at an accelerating voltage of 5 kV at a magnification scale of 50000x.

Impaction sampling was used for TEM analysis where the TEM grids (copper, 300 mesh, and lacey carbon film) holder is attached onto a gravimetric filter through which the exhaust sample passes in the existing PFDT system as used in [13,14]. A CM12 TEM (Philips, FEI Company, Netherlands) is used to examine the PM samples in this study. The TEM was operated at an accelerating voltage of 120 kV. TEM images were observed and digitized with the associated image acquisition system equipped with a Model 792 Bioscan digital camera (Gatan Inc., USA) and stored as 1024x1024 pixel computer images.

Digital images obtained by SEM and TEM are processed by using a public domain image processing and analysis program, ImageJ 1.38I [15]. Among the many features, the software yields the projected area, A_p, maximum projected length, L_{max}, maximum projected width, W_{max}, center of mass etc. It also provides best-fit ellipses to the particles's boundary and the corresponding major and minor diameter of the ellipses. Shape factor (SF) is then determined as the ratio of the minor to major axis of the ellipses fitting with the particles, and represents a measure of their shape. From the values of A_p, the projected area equivalent diameter, D_p, is determined which is defined as the diameter of a circle with the same area as the projected particle [16]. It is to be noted that the result presented for the number size distributions of the PM may not represent the actual particle size number concentration emitted by the engine as only a subset of the emitted particles is collected and observed on the SEM filter.

3. RESULTS AND DISCUSSIONS

3.1 Gaseous Emissions

3.1.1. NOx emissions

Figure 1(a) shows the results of NO_x emissions for the engine while operated at diesel and dual fuel modes. Significantly higher NO_x is formed during diesel high load operation compared to diesel light load. It is well known that the formation of NO_x is strongly dependent on temperature, the local concentration of oxygen and the duration of combustion [11,13,17]. In the case of diesel high load, high NO_x formation is mainly due to the high combustion temperature and the duration of combustion even though the oxygen availability is lower at high load compared to that in light load. However, from Fig.1(a), NO_x emissions are found to be reduced significantly for biogas fueling compared to diesel fueling. NO_x concentration is found to be decreased by about 13 to 37% during biogas fueling with increasing CO_2 contents compared with diesel fueling. Therefore, it is clear that these notable differences in NO_x concentrations are mainly due to the presence of CO_2 in biogas. CO_2, being a diluent, results in slower flame propagation and lowers the level of the cycle temperatures. In addition, increasing CO_2 in biogas also decreases oxygen in the charge. Hence, NO_x formation is suppressed with the combined effects of these phenomena in the case of biogas fueling [9].

3.1.2. HC emissions

Unburned hydrocarbon (HC) emissions are presented in Fig. 1(b) for different engine fueling. A similar or slightly higher HC concentration is found for diesel high load condition with compared to diesel light load. However, with the introduction of biogas, HC emissions increase sharply by more than three times compared to baseline diesel fueling. With the introduction of gaseous fuels, turbulent flame propagation from the ignition regions of the pilot is normally suppressed due to the lower temperature and air-fuel ratio and it will not proceed until the concentration of the gaseous fuel reaches a minimum limiting value. Also it is reported that the ignition is normally more delayed with dual fueling compared to diesel fueling [17]. In addition to the mechanisms, there are contributions from crevice volumes, which remain unburned. Valve overlapping between the intake and exhaust to facilitate scavenging can also cause an increase in HC emissions for dual fueling as it blows unburned gas-air mixture out of the cylinder [7]. When compared between different biogases, a mild increase in HC emissions is observed (Fig.1b) with the increase of CO_2 content in fuel. The presence of CO_2 in biogas slows down the overall combustion process and narrows down the effective flammability limits. These effects act more with increasing CO_2 contents. However, these effects are mostly compensated during operations with high load or high equivalence ratios, which are the cases of the present study. A similar observation for unburned methane concentrations in the exhaust is reported for methane-CO_2 fueling with varied CO_2 [3].

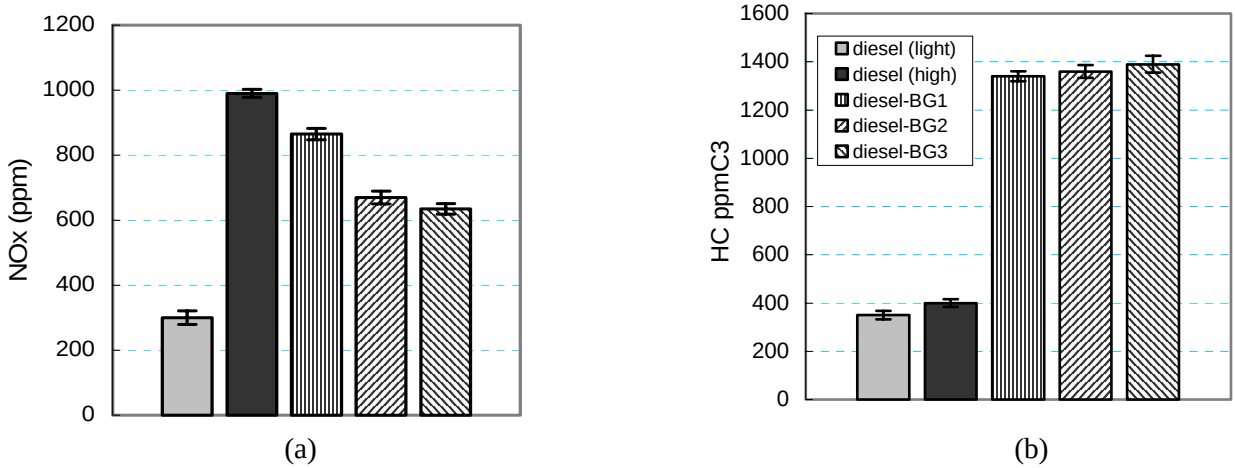

(a) (b)

Fig.1 (a) NO_x and (b) unburned HC concentrations in the exhaust for diesel and dual fueling (engine speed = 1750 rpm; torque = 3 Nm (diesel light load) and 28 Nm for others; injection at 28°btdc).

3.2. PM Emissions

3.2.1 Mass emissions

Figure 2 presents the PM mass concentrations (in brake-specific mass unit, g/kW-h) measured by the gravimetric method for diesel and dual fueling. The error bars in Fig.1 and 2 are for 2 standard deviation of the data measured at different times and days for the same operating conditions. Under light load condition, the PM emissions (per engine power output) are found to be the highest among all other operating conditions. A similar observation is reported by Ogawa et al. [14] for the light load operations with different diesel test fuels. The lower temperature in light load operations is the dominant factor for the high PM mass emissions. The exhaust temperature is observed as 198±2°C under light load compared to 455-485°C for high load operations. Therefore the major part of the heavy fraction of the hydrocarbons remains unburned which later condenses to be associated with the soot particles. As the load increases, the combustion temperature increases which enhances soot particle oxidation and the amount of unburned hydrocarbon decreases. As a result, the PM mass emissions reduce compared to the light load operations up to a certain fuel/air equivalence ratio. Beyond that the lack of oxygen causes increase in PM mass emissions. However, a significant reduction in PM emissions is found in the case of dual fuel operations compared to diesel operations. PM mass emissions are reduced by about 70 percent for dual fueling compared to diesel fueling under same operating conditions. Quantitatively similar results are reported by Boisvert et al. [6] and Zbaraza [18] for diesel-NG dual fuel operation. The results in Fig.2 also indicate that the quality of biogas has little or no impact on PM mass emissions at this particular engine operating condition. This can be explained that the formation of the majority of PM is caused by the liquid diesel, which is minimized in the case of dual fuel operations. On the other hand, as the engine is operated at high load, the combustion temperature remains similar to diesel high load operation. Therefore, the high temperature contributes to the oxidation of the generated soot particles from the minimum amount of liquid diesel. In addition, for diesel-biogas fueling, the combustion is more prolonged due to the presence of the diluent [3] and therefore provides more opportunities to oxidize the soot particles.

3.2.2 PM shape analysis

Figure 3 presents the shape factors (SF) of the measured PM for diesel and duel fueling. SF close to one indicates more rounds (spherical), than the particles having a shape factor close to 0.1 (12). The particles with SF close to 0.1 are therefore, long-chained or elongated. In the case of diesel light and dual fuel operations, the peaks are shifted towards the SF = 1.0, indicating the particles are more round (spherical) compared to the peak of diesel PM, which lies at around SF = 0.5. The SF for the majority of particles of dual fuel operations ranges between 0.65 and 0.7. This indicates that the PM measured in the case of dual fuel operations are more nearly spherical and less chainlike agglomerated compared to diesel (high) fueling. This can be observed qualitatively in Fig. A2 in the appendix.

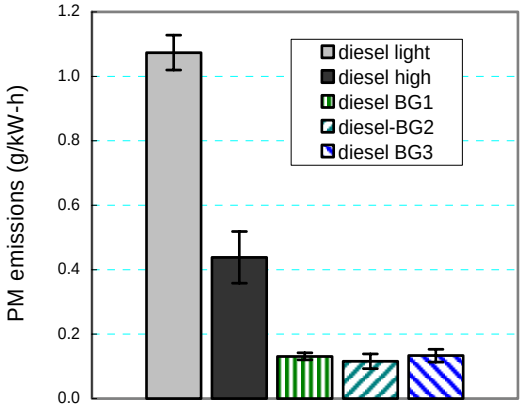

Fig.2 PM mass emissions by gravimetric method for diesel and dual fueling (engine speed = 1750 rpm; torque = 3 Nm (diesel light load) and 28 Nm for others; injection at 28°btdc).

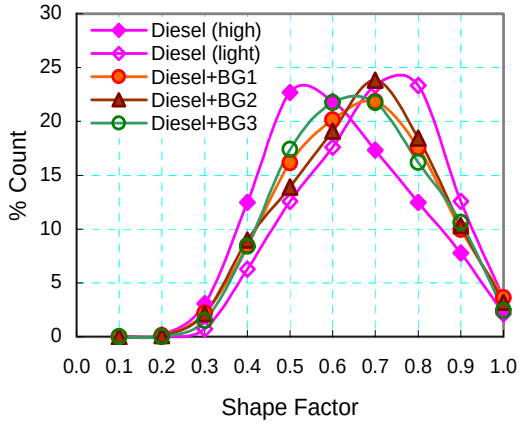

Fig.3 Shape factor (SF) trends of the PM collected on SEM filters for diesel and dual fueling (1750 rpm, and pilot = 0.6 kg/hr for dual fueling).

As previously mentioned, the major source of PM formation can be attributed to the liquid diesel. This is because of the large number of carbon molecules present in diesel compared to methane in the gaseous fuel. Also, increasing hydrogen in the gaseous fuel decreases the PM formation tendency [19]. Further the gaseous fuel does not contain polycyclic or aromatic compounds, which are precursors for PM formation. Formation and nucleation of particles from diesel combustion is followed by the surface growth where the gas-phase hydrocarbons, mostly acetylenes, are added to the particle nuclei. The particles with an increased mass then undergo further processes such as coagulation and agglomeration. In the coagulation processes, spherical particles collide with each other and coalesce and form a larger primary spherical particle. When the particle growth rate slows down, continued collision between the spherical primary particles results agglomeration to form large clusters of primary particles, which appears to be chain-like. The rate of agglomeration is proportional to the square of the primary particle number density [20]. As the number density of the primary particles formed in the case of diesel fueling is expected to be much higher than that of dual fuelling, the rate of chain-like agglomerated PM formation is also much higher in this case. Finally, the oxidation plays a significant role throughout the total processes of PM formation, which is more effective in the case of dual fueling to reduce the rate of formation of the agglomerated particles, and thus the total PM mass emissions are minimized.

3.2.2 TEM observation

PM agglomerates are observed at a high magnification on TEM. It can be observed from Fig.4 that the agglomerates are mainly composed of numerous individual spherical tiny particles. These particles are known as primary particles. With the help of image analysis software, the diameters of these primary particles can easily be analyzed. For diesel (high) load, the mean diameter of primary particles is found to be 26.3 nm and for dual fueling It varies between 27.5 to 29.5 nm indicating slightly larger primary particles are generated in the latter case.

4. CONCLUSIONS

The main objective of the present study is to compare the emissions (gaseous and PM) of a diesel engine operated on diesel and dual mode. No modifications were performed on the test engine to optimize its performance or emissions. Engine speed, output power and injection timing were the same for diesel high and the dual fuel operations. The following conclusions may be drawn from the results of the present study:

- Quite a stable engine operation at this load (~75% of the rated torque) and speed is possible with biogas fueling without any modifications either from the engine or the operational points of view.
- For biogas fueling NO_x emissions are lowered significantly (maximum by 37% compared to diesel fueling).

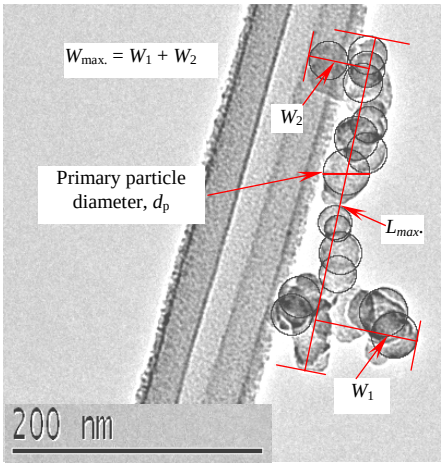

Fig.4 TEM micrograph showing the measurements of primary particle diameter in an agglomerate and the maximum projected length and width of the agglomerate.

- PM mass emissions are reduced substantially in the case of dual fueling irrespective of its quality. About 70% in PM emissions are obtained in this study.
- SEM analysis on collected PM indicates that dual fuel PM are smaller and rounder than diesel PM.
- TEM observation shows that the PM agglomerates are mainly composed of numerous nanometer size primary particles (<30nm). Diesel (high) PM has slightly smaller primary particles than that of dual fuel PM.

5. REFERENCES

[1] Park K., Kittelson D. B. and McMurry P. H., Structural Properties of Diesel Exhaust Particles Measured by Transmission Electron Microscopy (TEM): Relationships to Particle Mass and Mobility, *Aerosol Science and Technology*, 38(2004), pp. 881–889.

[2] Papagiannakis R. G. and Hountalas D. T., Combustion and Exhaust Emission Characteristics of a Dual Fuel Compression Ignition Engine Operated with Pilot Diesel Fuel and Natural Gas, *Energy Conversion and Management*, 45(2004), pp. 2971-2987.

[3] Karim G. A. and Wierzba I., Methane-Carbon Dioxide Mixtures as a Fuel, SAE Paper 921557, 1992.

[4] Karim G. A., A Review of Combustion Processes in the Dual Fuel Engine - The Gas Diesel Engine, *Progress in Energy and Combustion Science*, 6(1980), pp. 277-285.

[5] Selim M.Y.E., Effect of Engine Parameters and Gaseous Fuel Type on the Cyclic Variability of Dual Fuel Engines, *Fuel*, 84(2005), pp. 961-971.

[6] Boisvert J., Gettel L.E. and Perry G.C., Particulate Emissions for a Dual-Fuel Caterpillar 3208 Engine, ASME Paper 88-ICE-18, 1988, pp. 277-285.

[7] Weaver C.S. and Turner S.H., Dual Fuel Natural Gas/Diesel Engines: Technology, Performance, and Emissions. SAE Paper 940548, 1994.

[8] Patterson J., Clarke A. and Chen R., Experimental Study of the Performance and Emissions Characteristics of a Small Diesel Genset Operating in Dual-Fuel Mode with Three Different Primary Fuels, SAE Paper 2006-01-0050, 2006.

[9] Karim G.A. and Amoozegar N., Examination of the Performance of a Dual Fuel Diesel Engine with Particular Reference to the Presence of Some Inert Diluents in the Engine Intake Charge, SAE Paper 821222, 1982.

[10] Burtscher H., Physical Characterization of Particulate Emissions from Diesel Engines: A Review, *Journal of Aerosol Science*, 36(2005), pp. 896-932.

[11] Heywood, J. B., Internal Combustion Engine Fundamentals, McGraw – Hill, New York, 1988.

[12] Nord K., Haupt D., Ahlvik P., Egeback K-E., Particulate Emissions from an Ethanol Fuelled Heavy-Duty Diesel Engine Equipped with EGR, Catalyst and DPF, SAE Paper 2004-01-1987, 2004.

[13] Stone R., Introduction to Internal Combustion Engines, SAE Inc., Warrendale, PA, 1999.

[14] Ogawa T., Nakakita K., Yamamoto M., Okada M. and Fujimoto Y., Fuel effects on particulate emissions from D.I. engine - Relationship among diesel fuel, exhaust gas and particulates, SAE Paper 971605, 1997.

[15] Rasband W.S., ImageJ, US National Institutes of Health, Bethesda, MD, USA, <http://rsb.info.nih.gov/ij/>, 1997–2006.

[16] Hinds W. C., Aerosol Technology, Properties, Behavior, and Measurement of Airborne Particles, J. Wiley and Sons, Inc., New York, 1999.

[17] Karim G.A., Combustion in Gas Fueled Compression: Ignition Engines of the Dual Fuel Type, *Journal of Engineering for Gas Turbines and Power*, 125(2003), pp. 827-836.

[18] Zbaraza D., Natural Gas Use for On-Sea Transport, Diploma Thesis, University of Science and Technology Krakow, Poland, 2004.

[19] Tree D.R. and Svensson K.I., Soot Processes in Compression Ignition Engines, *Progress in Energy and Combustion Science*, 33(2007), pp. 272-309.

[20] Smith O.I., Fundamentals of Soot Formation in Flames with Application to Diesel Engine Particulate Emissions, *Progress in Energy and Combustion Science*, 7(1981), pp. 275-291.

Appendix

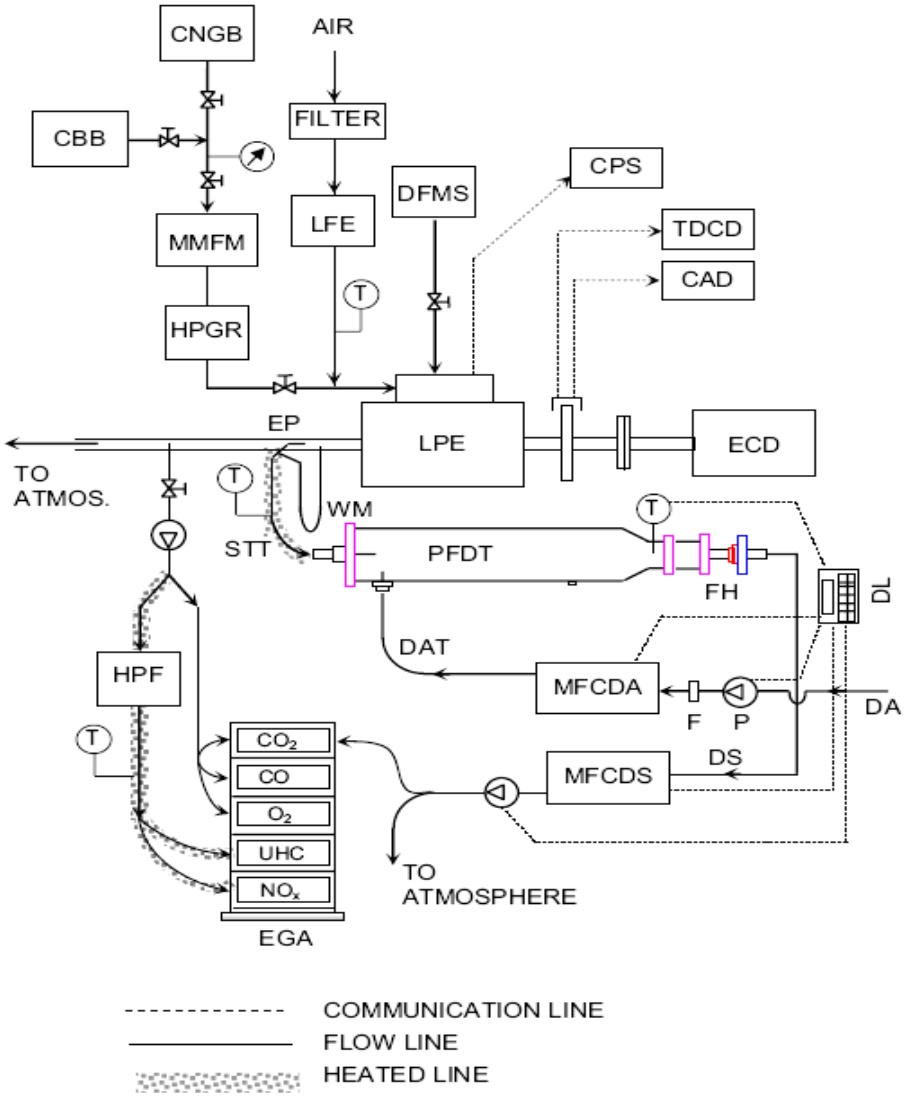

CAD = CRANK ANGLE DECODER; TDCD = TDC DETECTOR
CBB = COMPRESSED BIOGAS BOTTLE
CNGB = CNG BOTTLE
CPS = CYLINDER PRESSURE SIGNAL
DATT = DILUTION AIR TO TUNNEL; T = THERMOCOUPLE
DFMS = DIESEL FLOW MEASURING SYSTEM
DL = DATA LOGGER; DA = DILUTION AIR
DT = DUST TRAK™; DS = DILUTED SAMPLE
ECD = EDDY CURRENT DYNAMOMETER
EP = EXHAUST PIPE; EGA = EXHAUST GAS ANALYZERS
FH = FILTER HOLDERS; F = FILTER; P = PUMP
HPR = HIGH PRESSURE GAS REGULATOR
LFE = LAMINAR FLOW ELEMENT
LPE = LISTER PETTER ENGINE
MFCDA = MASS FLOW CONTROLLER FOR DILUTION AIR
MFCDS = MASS FLOW CONTROLLER FOR DILUTED SAMPLE
MMFM= MICRO-MOTION® MASS FLOW METER
P = PUMP
PFDT = PARTIAL FLOW DILUTION TUNNEL
STT = SAMPLE TRANSFER TUBE
T = TEMPERATURE SENSOR
WM = WATER MANOMETER; HPF = HEATED PREFILTER

Fig.A1 Schematic diagram of the experimental setup.

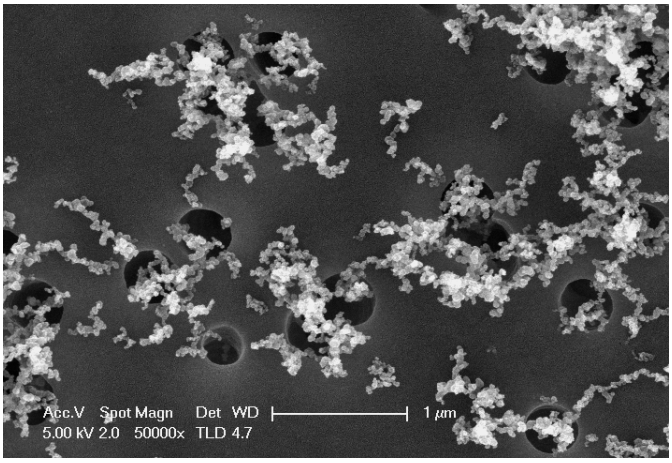

(a)

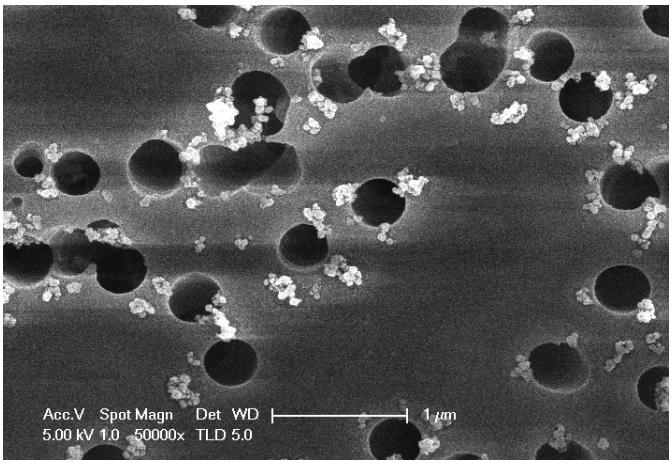

(b)

Fig.A2 SEM images for (a) diesel high (more chain-like agglomerates) and (b) diesel-biogas (smaller and nearly spherical agglomerates) operations (torque = 28 Nm, speed = 1750 rpm, diesel pilot for dual fuel = 0.6 kg/hr; the black circles are the pores in the filter with a nominal diameter of 0.4μm).

528

Proceedings of the 4th BSME-ASME International Conference on Thermal Engineering
27-29 December, 2008, Dhaka, Bangladesh

FINITE-TIME THERMODYNAMIC MODELLING AND SIMULATION OF IRREVERSIBLE DIESEL CYCLE ENGINES

P. C. Roy

Department of Mechanical Engineering,
National Institute of Technology Silchar
Silchar, Assam, India
E-mail:prokash@nits.ac.in or prokash.roy@gmail.com

ABSTRACT

A finite-time thermodynamic modelling and simulation of irreversible Diesel cycle engines has been developed considering non-linear variable specific heats with temperature, heat transfer loss, internal irreversibility effects and engine friction loss. A parametric study on performance characteristics such as power and efficiency have been made and discussed which may be used in actual engine designs and applications. Effect of engine speed, heat transfer loss, and internal irreversibility with respect to compression ratio on power and cycle efficiency have been analysed and discussed.

Key words: *Irreversible Diesel cycle, variable specific heats, engine losses, performance.*

1. INTRODUCTION

The accurate analysis of the various processes in an internal combustion engine is a very complex problem. The accurate analysis can be obtained experimentally when it will be carried out correctly and systematically. But it would be time consuming and very expensive. Theoretical analysis is an alternative option to study the engine operation without actually building and physically testing an engine. Theoretical analysis involves modelling and simulating of the engine operation with the help of thermodynamics to form mathematical expressions which is solved in order to obtain the relevant desired output parameters. It is obvious that the method of solution will depend upon the complexity of the formulation of the mathematical expressions which in turn will depend upon the assumptions that have been introduced in order to analyze the processes in the engine. The more the assumptions, the simpler will be the mathematical expressions and the easier the calculations, but the lesser will be the accuracy of the final results.

Air standard cycle is often used as ideal cycle for internal combustion engine. In that case, air is assumed to behave as an ideal gas, and all processes are considered to be reversible, there is no losses from system to the surroundings, specific heats of gas are also kept constant though they change with temperatures [1-2]. In actual practice, it is unrealistic. But it is the most simplified cycle to understand the major thermodynamic processes occurring in internal combustion engines and it provides approximation on trends of power output and cycle efficiency.

In the irreversible cycle, most of the losses are encountered to achieve nearly actual cycle efficiency obtained in experimental analysis. During the last decade, many researchers are working to analysis irreversible internal combustion engine cycle incorporating different losses with some assumptions [3, 20].

The effect of heat transfer losses in the net power out put and efficiency on different air standard cycle have been analysed and discussed by many researcher [2-3,6] to understand the effect neglecting the other engine losses. But in the actual engine operation, friction has a significant effect on the performance. Bhattacharya (2000) [5] optimized an irreversible Diesel cycle by fine tuning of compression ratio and cut-off ratio considering global thermal and friction losses lumped into an equivalent friction term. Chen et al. (2002) [7] also analysed the friction effects on the characteristic performance of Diesel engines. Similarly, Wang et al. (2002) [8] extended the study to see the effects of friction on the performance dual cycles. Later on, Chen et al. (2003) [9] derived the characteristics of power and efficiency for Otto cycles to see the effect of both heat transfer and friction losses. They also extended to find optimal performance based on the both effects for irreversible dual cycles (2004) [10]. Chen et al. (2005) [11] analyzed and optimized the finite-time thermodynamic performance of an air-standard Otto cycle considering heat transfer and friction-like term losses. Ge et al. (2005) [12] developed generalized irreversible reciprocating heat-engine cycle model with heat-transfer loss and friction-like term loss was analyzed using finite-time thermodynamics.

The studies mentioned above were based on the constant specific heats of the working fluid. But in actual practice, specific heats of the fluid changes with the change in temperature and effect of specific heats

should be considered in actual cycle analysis. Ge et al. (2005) [13] done thermodynamic simulation of performance of an Otto cycle with the consideration of heat transfer loss and variable specific heats.
Abu-Nada et al. (2006) [14]done a thermodynamic modelling of spark-ignition engine to investigate the effect of temperature dependent specific heats and compared to that which uses constant temperature specific heats. Al-Sarkhi et al. (2006) [15] studied the effect friction and temperature dependent specific heat of the working fluid on the performance of a Diesel-engine. Ge et al. (2006) [16] modified their thermodynamic simulation to see the effect of heat transfer loss, friction and variable specific heats of working fluids on the performance of an irreversible dual cycle. Chen et al. (2006) [17] studied the effects of heat transfer, friction and variable specific heats of working fluid on performance of an irreversible dual cycle. Ozsoysal (2006) [18] pointed out some of the limitations regarding the consideration of heat transfer loss taken by the earlier researchers. He suggested a more realistic and precise relationship between the fuel's chemical energy and the heat leakage needs to be derived through the resulting temperature and found more realistic and valid range of the heat loss parameter and the fuel's energy. Lin et al. (2008) [19] emphasized the performance of air standard Otto cycle with considerations of variable specific heats of the working fluid, friction and heat leakage characterized by a percentage of the fuel's energy. Ge et al. (2008) [20] done finite-time thermodynamic modelling and analysis of an irreversible Otto cycle considering the effect of internal irreversibility, heat transfer loss and friction loss on the cycle performance.

In the view of the above literatures, it has been found that effect of various losses on the cycle efficiency and power output have been analysed and discussed at different compression ratios and compared their effects on power and cycle efficiency. But details parametric studies on irreversible cycle, considering all the loss effects are not reported. Keeping view on the above literature, finite-time thermodynamic modelling and simulation of irreversible Diesel cycle has been done keeping the maximum temperature of the cycle is constant which may be fixed with the metallurgical considerations. Individual effects of variable non-linear specific heats with temperature, friction losses and heat transfer losses have been shown in the present model. Effects of internal irreversibility in compression and expansion have been depicted. Combined effect of engine speed, heat transfer loss, and internal irreversibility with respect to compression ratio on thermal efficiency have been analysed and discussed.

2. MODEL FORMULATION

An irreversible air standard cycle model, which is consists of four processes (1-2: compression process, 2-3: heat addition process, 3-4: expansion process and 4-1: heat rejection process) for Diesel cycle has been shown in figure 1. Figure 1. (a) and (b) represents the P-v and T-s diagram of the respective processes. In the present model, heat addition to the cycle has been varied with the change of compression ratio such that maximum temperature of the cycle will be remaining unchanged shown in figure 1. (b).

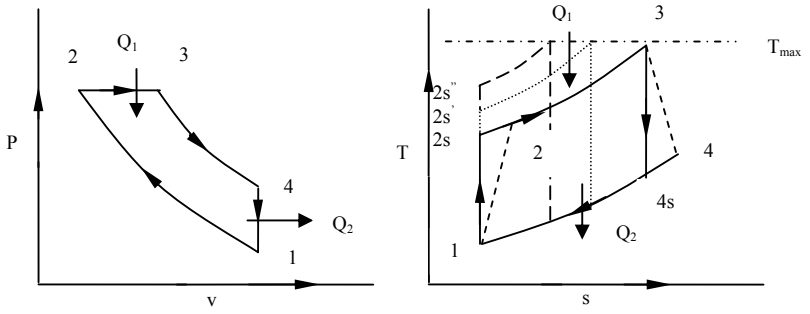

Figure 1. (a) P-v and (b)T-s diagram of Diesel cycle.

For ideal air standard Diesel cycle heat added to the cycle take place at constant pressure and heat rejection takes place at constant volume process as follows.

Heat added to the cycle, $q_1 = q_{23} = c_p(T_3 - T_2)$ (1)

Heat rejected from the cycle, $q_2 = -q_{41} = c_v(T_4 - T_1)$ (2)

Then the air-standard cycle efficiency becomes, $\eta_{as} = \frac{w_{net}}{q_1} = 1 - \frac{q_2}{q_1}$ (3)

In ideal cycle, specific heats of the working fluid are assumed as constant though this assumption is valid for small temperature differences. But in actual practice there is a large temperature difference during one complete cycle. We have used a non-linear relation of specific heats at constant pressure with temperature range of 300K to 3500K [14, 20] which can be written as

$$c_p = 2.506\times10^{-11}T^2 + 1.454\times10^{-7}T^{1.5} - 4.246\times10^{-7}T + 3.162\times10^{-5}T^{0.5} \quad (4)$$
$$+1.3303 - 1.512\times10^{4}T^{-1.5} + 3.063\times10^{5}T^{-2} - 2.212\times10^{7}T^{-3}$$

Specific heats at constant volume can be obtained by; $c_v = c_p - R$ Where R is the gas constant of the working fluid.

So, heat added and rejected from the cycle can be obtained by

$$Q_1 = m\int_{T_2}^{T_3} c_p dT \quad (5)$$

$$Q_2 = m\int_{T_1}^{T_4} c_v dT \quad (6)$$

For ideal cycle, process (1-2) is considered as a reversible isentropic process, in the present work, internal irreversibility of the compression and expansion processes has been considered as compression and expansion efficiency terms as follows,

For compression process, $\eta_c = \frac{T_{2s} - T_1}{T_2 - T_1}$ (7)

For expansion process, $\eta_e = \frac{T_3 - T_4}{T_3 - T_{4s}}$ (8)

Since c_p and c_v are dependent on temperature, ratio of specific heats (k) also varies with temperature so constant value of k can not be used. A suitable engineering approximation has been utilized for reversible adiabatic process with variable k [15, 20]. Any reversible process between i and j has considered a large numbers of infinitesimally small processes with constant k. In that case infinitesimally small change in temperature *dT* and volume *dV* of the working fluid takes place which may be represented as

$$TV^{k-1} = (T + dT)(V + dV)^{k-1} \quad (9)$$

Neglecting the higher order terms, eq. (9) becomes, $c_v \ln\frac{T_j}{T_i} = R\ln\frac{V_i}{V_j}$ (10)

Where the temperature in the equation of c_v is $T = (T_j - T_i)/\ln\frac{T_j}{T_i}$ (11)

And $\frac{V_i}{V_j}$ is define as compression ratio, r. With this above approximation, reversible adiabatic processes of the model can be represented as, for compression process, $c_v \ln\frac{T_{2s}}{T_1} = R\ln(r/r_c)$ (12)

and for expansion process $c_v \ln\frac{T_{4s}}{T_3} = -R\ln r_e$ (13)

Where, r_c and r_e are cut off ratio and the expansion ratio of the cycle.

In actual cycle operation there will be certain heat loss from system to the surroundings due to finite temperature differences between working fluid and cylinder wall. Heat transfer loss through the cylinder wall has been assumed to be proportional to the average temperature of heat addition and cylinder wall temperature which is represented by [20].

$$Q_{HL} = mB(T_2 + T_3 - 2T_0) \quad (14)$$

Where, B is a constant related with heat transfer and T_0 is the cylinder wall temperature. This idealization is more realistic because heat loss will be more when there is more mean temperature of heat addition assuming constant cylinder wall temperature.

Loss due to piston friction has been considered assuming a dissipation term which represented by friction force which is in linear function of mean piston velocity gives as [20]

$$f_\mu = \mu v = \mu\frac{dx}{dt} \quad (15)$$

where, μ is a coefficient of friction which takes into account the global losses and x is the piston displacement. So power loss due to friction can be obtained by,

$$P_\mu = \frac{dW_\mu}{dt} = \mu\frac{dx}{dt}\frac{dx}{dt} = \mu v^2 \quad (16)$$

Mean piston speed can be obtained for four stoke cycle engine by $v = 4LN$ (17)
Where, L is the stroke length of the cylinder and N is the speed of the engine in rps.

Therefore, net power out of the cycle can be obtained by,
$P_{net} = Q_1 - Q_2 - P_\mu$ (18)
The efficiency of the cycle is
$$\eta = \frac{P_{net}}{Q_1 + Q_{HL}} \quad (19)$$

Solving methodology:
For a particular engine, value of initial temperature and maximum temperature, T_1 and T_3, compression ratio, r and η_c and η_e are given. T_{2s} can be obtained from eq. (12) but need an initial value of c_v. After getting the value of T_{2s}, calculate T for getting a new value of c_v by eq. (4) and find final T_{2s} by iterative scheme. T_2 can be obtained by eq. (7). Similarly T_4 can be obtained. Amount of heat transfer loss and friction loss are obtained from eq. (14) and eq. (15) respectively. Finally power output and efficiency of the cycle can be calculated using eq. (18) and (19) respectively. Cut of ratio, r_c, is obtained by equation of state,
$r_c = \frac{V_3}{V_2} = \frac{T_3}{T_2}$ since, heat added at constant pressure.

3. RESULTS AND DISCUSSIONS
Detailed parametric studies such as effect of non-linear variable specific heats, effect of heat transfer loss, effect of internal irreversibility, effect of friction loss as well as combined effect of all have been made based on the model data used [20] as follows.

3.1 Effect of specific heats
In the figure 2. (a), it has been found that with the increase in CR, T_2 has been increased and corresponding values of c_v and c_p have been increased but ratio k has been decreased. But in case of expansion process, reverse phenomenon has been depicted in figure 1 (b). Changes in c_v, c_p and k have significant impact on the performance of the engine cycle.

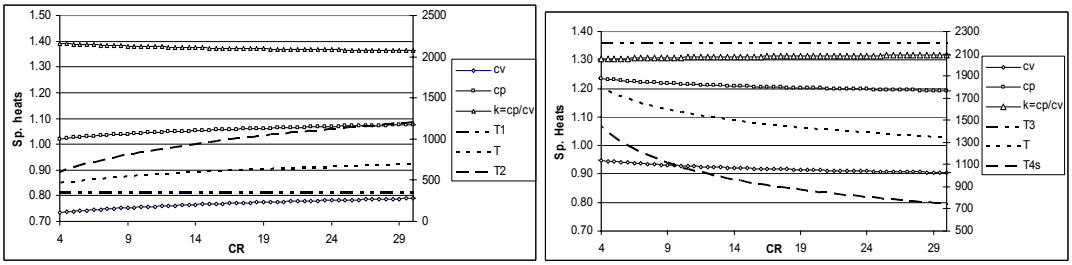

(a) (b)

Figure 2. Variation of temperature, cp, cv and k during (a) adiabatic compression and (b) expansion processes at different CR

3.2 Effect of heat transfer loss
Effect of heat transfer loss on power and efficiency has been shown in figure 3. It has been found cycle efficiency decreases sharply when losses increase from B=100J/kg to 200J/kg. Here B term is related with the heat transfer such as conductivity etc.

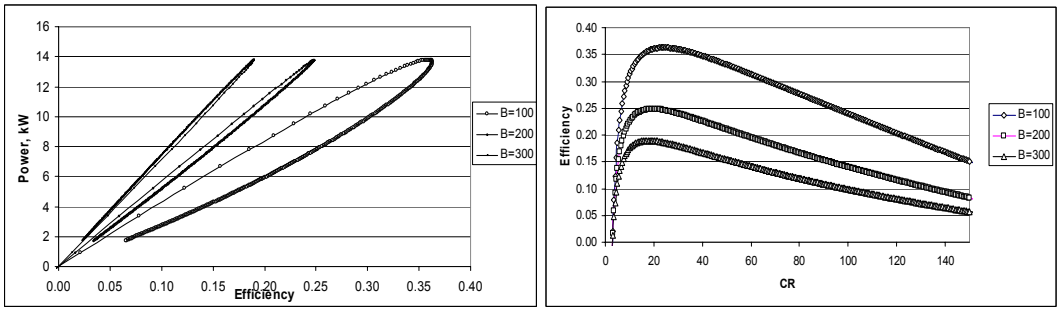

Figure 3. Power and efficiency characteristics at different value of heat transfer loss for Diesel engine.

3.3 Effect of internal irreversibility

With the increase in internal irreversibility at the compression and expansion process, decreases the cycle efficiency shown in figure 4. But actual practice there have some internal irreversibility, so loop form in the power efficiency characteristics is desirable.

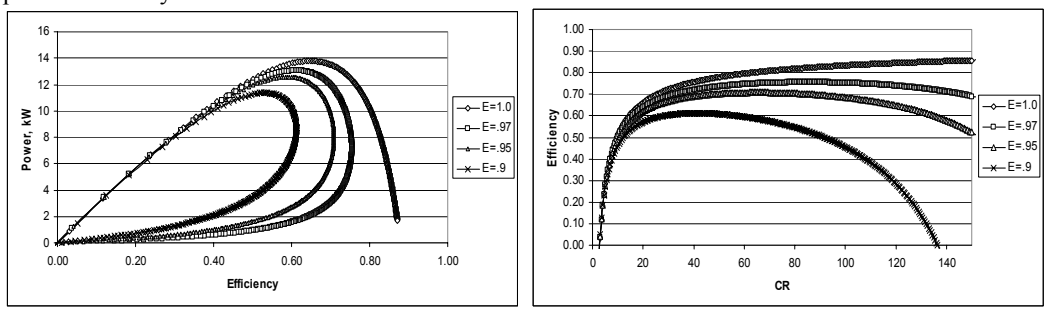

Figure 4. Power and efficiency characteristics at different value at different internal irreversibility

3.4 Effect of friction

Effect of engine piston friction is related with the engine speed. Efficiency of the cycle decrease when engine friction increases shown in figure 5. But in actual practice engine frictional loss is reduced by providing adequate lubrication and piston rings.

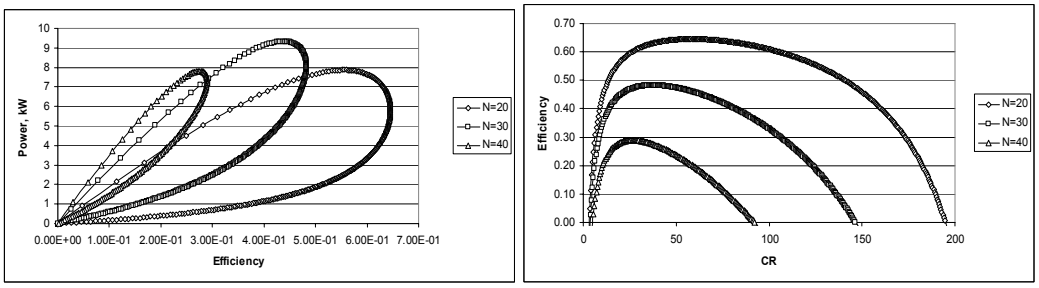

Figure. 5 Effect of friction on cycle performance

3.5 Combined effects of losses.

Combined effect of all the losses discussed above, have been depicted below at different value of internal irreversibility shown in figure 6. Though for the parametric analysis, it has been used some arbitrary values of different losses. But there are a certain ranges of compression ratio where cycles provide maximum cycle efficiency that lies between 14 and 30 which have been found in most of the actual Diesel engines.

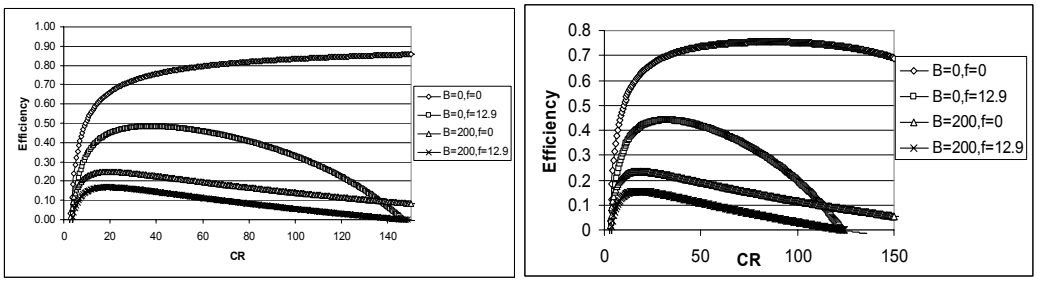

Figure 6. Effect of different losses when there is no internal irreversibility (E=1) and with an internal irreversibility. (E=0.97)

4. CONCLUSIONS

A finite-time thermodynamic modelling and simulation of irreversible Diesel cycle engines has been developed considering non-linear variable specific heats with temperature, heat transfer loss, internal irreversibility effects and engine friction loss. It has been found that there is a distinct change in specific heats as well in its ratio at the time of compression and expansion processes and based on that performance of the cycle decreases. Cycle efficiency also decreases with the increase in other losses such that heat transfer, friction and loss due to internal irreversibility. Though for the parametric analysis, it been used some arbitrary values of different losses, but from the combined analysis of all the losses, it has been found that there have a certain ranges of compression

ratio where the Diesel cycles are getting maximum cycle efficiency that lies between 14 and 30 which have been found in most of the actual Diesel engines. With the incorporation of the actual engine dimensions and parameters, it can be obtained performance of the Diesel cycle close to the actual which have a practical importance in engine design.

REFERENCES

[1] Bejan, Advanced Engineering Thermodynamics, John Wiley & Sons, New York, 1988.
[2] Heywood JB. Internal combustion engine fundamentals. New York: McGraw-Hill; 1997.
[3] Chen L, Zen F, Sun F, Wu C. Heat transfer effects on the net work output and power as function of efficiency for air standard Diesel cycle. *Energ Int J* 1996; 21(12):1201–5.
[4] Chen L, Wu C, Sun F, Cao S. Heat transfer effects on the net work output and efficiency characteristics for an air standard Otto cycle. *Energ Convers Manage* 1998; 39(7):643–8
[5] Bhattacharyya, S. Optimizing an irreversible Diesel cycle−fine tuning of compression ratio and cut-off ratio, *Energy Convers. Mgnt.* 41 (2000) 847–854.
[6] Akash, B.A. Effects of heat transfer on the performance of an air-standard Diesel cycle, *Internat. Comm. Heat Mass Transfer* 28 (2001) 87–95.
[7] Chen L, Lin J, Luo J, Sun F, Wu C. Friction effects on the characteristic performance of Diesel engines. *Int J Energ Res* 2002;26(10):965–71.
[8] Wang W, Chen L, Sun F, Wu C. The effects of friction on the performance of an air standard dual cycle. *Exergy An Int J* 2002;2(4):340–4.
[9] Chen L, Zheng T, Sun F, Wu C. The power and efficiency characteristics for an irreversible Otto cycle. Int J Ambient Energ 2003;24(4):195–200.
[10] Chen L, Sun F, Wu C. The optimal performance of an irreversible dual cycle. *Appl Energ* 2004; 79(1):3–14.
[11] Chen, J. Zhao, Y He,. J. Optimization criteria on the important parameters of an irreversible Otto heat engine, *Appl. Energy* 83 (2005) 228–238.
[12] Ge, Y. Chen, L., Sun, F. and Wu, C. Reciprocating heat-engine cycles *Applied Energy* 81 (2005) 397–408
[13] Ge Y, Chen L, Sun F, Wu C. Thermodynamic simulation of performance of an Otto cycle with heat transfer and variable specific heats of working fluid. *Int J Therm Sci* 2005; 44(5):506–11.
[14] Abu-Nada E, Al-Hinti I, Al-Aarkhi A, Akash B. Thermodynamic modelling of a spark-ignition engine: effect of temperature dependent specific heats. *Int Comm Heat Mass Transfer* 2006;32(8):1045–56.
[15] Al-Sarkhi A, Jaber JO, Abu-Qudais M, Probert SD. Effects of friction and temperature-dependent specific-heat of the working fluid on the performance of a Diesel-engine. *Appl Energ* 2006; 83:153–65.
[16] Ge Y, Chen L, Sun F, Wu C. Effects of heat transfer, friction and variable specific heats of working fluid on performance of an irreversible dual cycle. *Energ Convers Manage* 2006;47: 3224–34.
[17] Chen, L., Ge,, Y. Sun, F. Wu, C. Effects of heat transfer, friction and variable specific heats of working fluid on performance of an irreversible dual cycle, *Energy conversion Management* 47 (2006) 3224–3234.
[18] Ozsoysal OA. Heat loss as a percentage of fuel's energy in air standard Otto and Diesel cycles. *Energ Convers Manage* 2006;47:1051–62.
[19] Lin, J. Hou S., Effects of heat loss as percentage of fuel's energy, friction and variable specific heats of working fluid on performanceof air standard Otto cycle, *Energy Conversion and Management 49* (2008) 1218–1227
[20] Ge, Y. Chen L. Sun. F. Finite-time thermodynamic modelling and analysis of an irreversible Otto-cycle, Applied Energy 85 (2008) 618–624

STUDIES ON THE NOISE LEVEL AND PERFORMANCE OF A TWO CYLINDER DIESEL ENGINE USING MODIFIED MUFFLER.

Bankim Bihari Ghosh,Principal, IEM Salt lake, Kolakta,India and Research consultant,IIT, Kgp Rajsekhar Panua,Paritosh Bhattacharya, CEM,Kolaghat, Midnapore, India, Prabir Kumar Bose, Jadavpur University, Kolkata-32, India, Satyajit Chakraborty, Director, IEM, Salt Lake, Kolkata

ABSTRACT:

Pollution free environment is the demand of today's society. Noise pollution is one of the major environmental pollutants. The noise pollution affects human beings physically and psychologically. It leads to mental fatigue. I.C Engines are powerful source of noise. I.C. Engines are either gasoline or diesel engines and they differ in their noise characteristics. The principle sources of noise in both the types of engines are same. The principle sources of noise in automotive engines are intake noise, radiator noise, combustion noise etc. Out of these exhaust noise is predominant and it is to be controlled. A recent survey shows that even though heavy commercial trucks comprise only 5% of vehicle pollution. The truck comprises of 17% of transport pollution. Exhaust mufflers have received most attention from researchers because; exhaust muffler is the only remedy to control the exhaust noise of the engine. The present work aims the attenuation of sound by well design exhaust muffler and studies on the performance of the engine with modified designed muffler and existing muffler at different rpm 1200, 1300, 1400, and 1500. It is observed that the sound level at all rpm decreases 15 dB approximately. The performance characteristic is almost comparable.

KEYWORD:

Wave equation, Separable variable, Muffler

NOMENCLATURE:

L	Length of the muffler (m)
BSFC	Brake Specific Fuel Consumption
db	Decibel
f	Frequency
SPL	Sound Pressure Level
ω	Angular Velocity
t	Time (Second)

INTRODUCTION:

Pollution free environment is the demand of today's society. Noise pollution is one of the major environmental pollutants. The noise pollution affects human beings physically and psychologically. Noise is relative term. Play of music by some one may be noise for others. Automotive engines are main contributors for air and noise pollution in the metropolitan cities. If it is not controlled, majority of pollution will go deaf or half deaf in coming years. I.C Engines are powerful source of noise. I.C. Engines are either gasoline or diesel engines and they differ in their noise characteristics. The principle sources of

noise in both the types of engines are same. An ideal muffler of an IC Engine is expected to have the desired qualities like complete noise control, no resistance to the engine exhaust, very small size, suitable shape, very cheap. It is practically impossible for any muffler to satisfy all the above requirements. The main objective of the muffler is the noise reduction with practically having small resistance. The engine exhaust has its noise character with spectrum range from 2 Hz to 10000Hz, depending on the engine speed load and many others variables.

DESIGN AND FABRICATION:

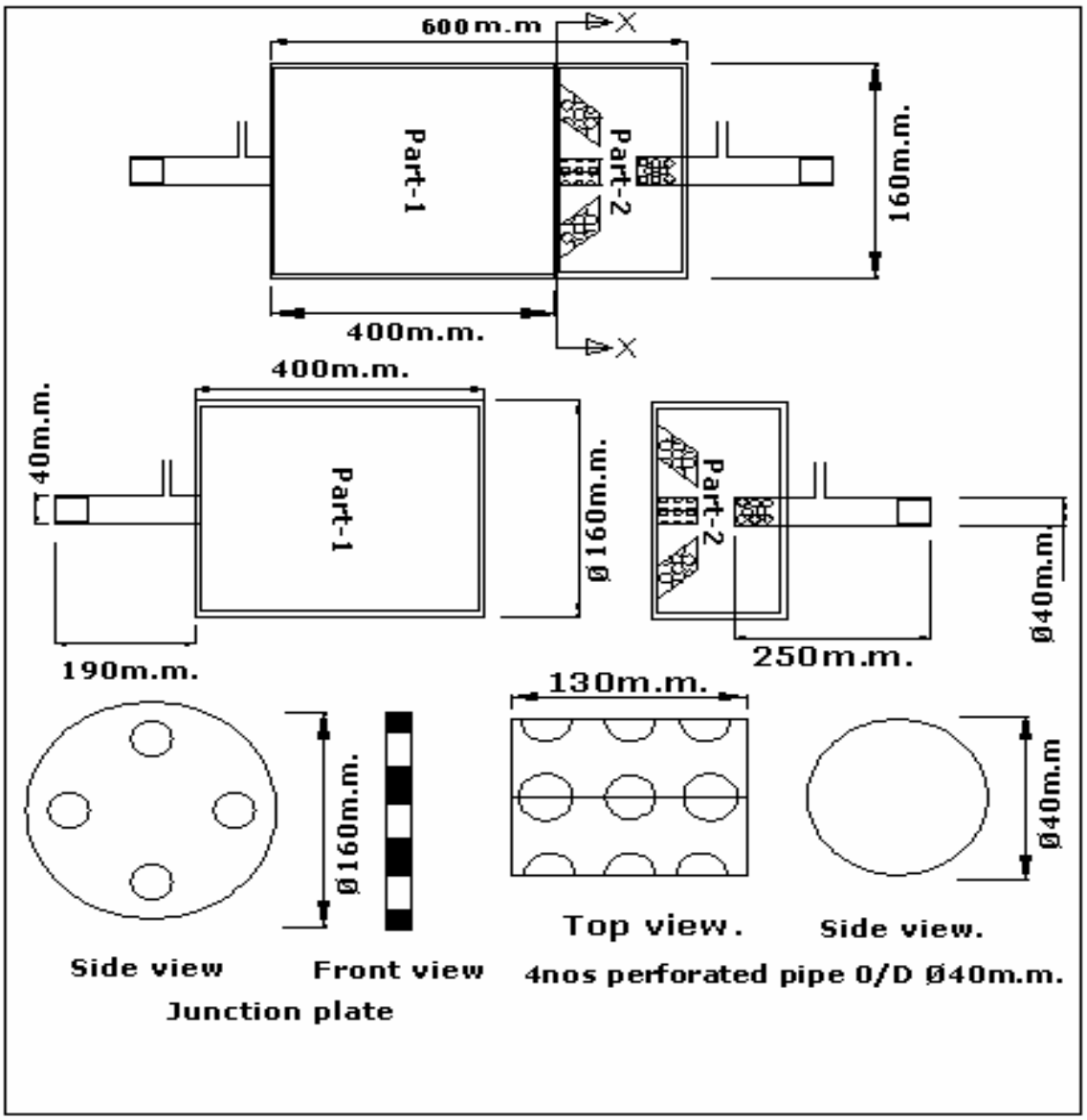

Fig.-1: DESIGN AND FABRICATION:

The reactive part of a muffler has been designed. In the beginning most of the flow transmitted as zero mode flow. Pattern of zero mode flow can be taken as mean flow. This indicates that sound pressure level (S.P. L) is maximum at the time of beginning of flow and gradually decays.

For resonative part of muffler number of hole are equal to 125 and of diameter is equal to 10mm each. These holes are arranged 25 numbers on each of four inlet pipes and one outlet extended pipe. These holes are arranged in 5 rows and 5 columns. For each inlet resonator pipe one row of holes are drilled near the end of pipe. Each resonator pipe is placed at angle 30^0 with H.P. with no baffles. It is desirable to have the resonator section near the inlet of the entire muffler system. The resonative part of muffler is modified by designing it as a two pass muffler having inlet and outlet pipes opposite to each other. These pipes are arranged with some eccentricity. The muffler gives Helmholtz resonative effect due to side branch resonator. There is no obstruction in the path of the exhaust gas i.e. baffles are not provided. This gives the effect of straight through muffler. The sound waves cancellation is more effective due to two pass of muffler.

EXPERIMENTAL SETUP:

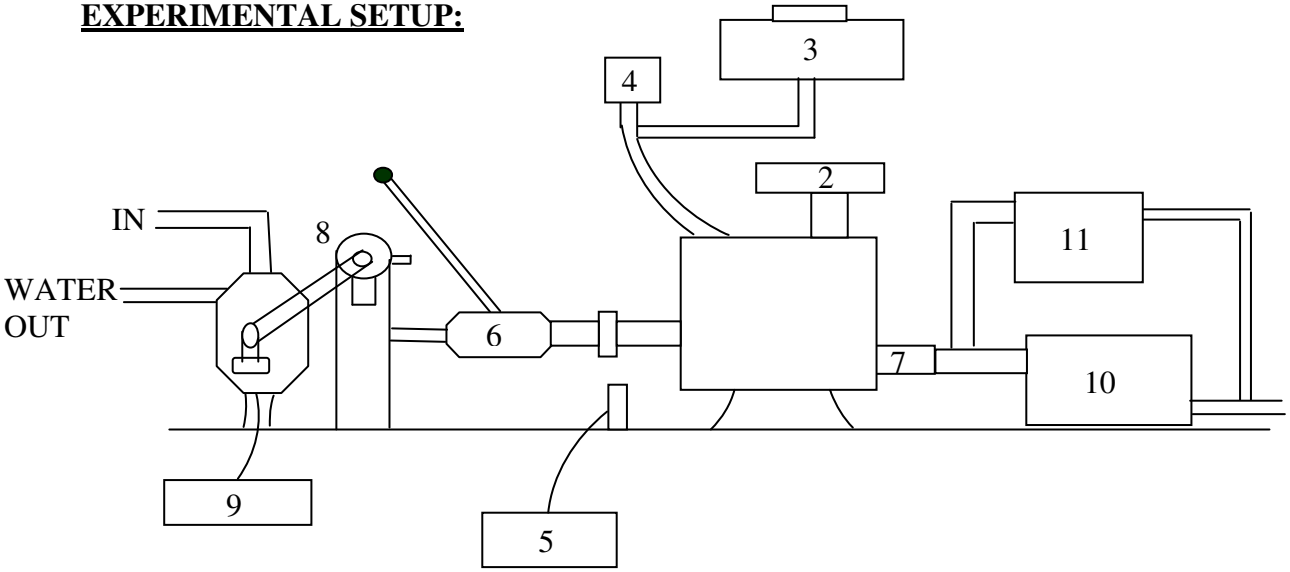

Fig.-2: EXPERIMENTAL SETUP:

1. ENGINE
2. AIR FILTER
3. DIESEL TANK

4. DIESEL MEASURING BURRET
5. SPEED INDICATER
6. CLUTCH
7. EXHAUST PIPE
8. ALTERNATOR
9. REACTIVE-RESONATIVE MUFFLER
10. MANOMETER

RESULTS AND DISCUSSION:

The experimental data are taken at various loads and various speeds. The engine speed varies from 1200rpm to 1500 rpm in the steps of 100rpm. These are rotational speeds with which loaded vehicles are plying on the road. The normal speed of the vehicle is assumed in the range of 40km/hr to 60 km/hr on the average road condition.

Figure 3 shows graph of break thermal efficiency Vs BP at 1200 rpm. It is found that there is a considerable loss of power due to modified muffler. The maximum break thermal efficiency of the engine with modified muffler is 23.25% which is 0.45% lower than existing muffler and 2.55% lower than the performance of the engine when it was tested without muffler because of little higher back pressure in comparison to the existing muffler and without muffler.

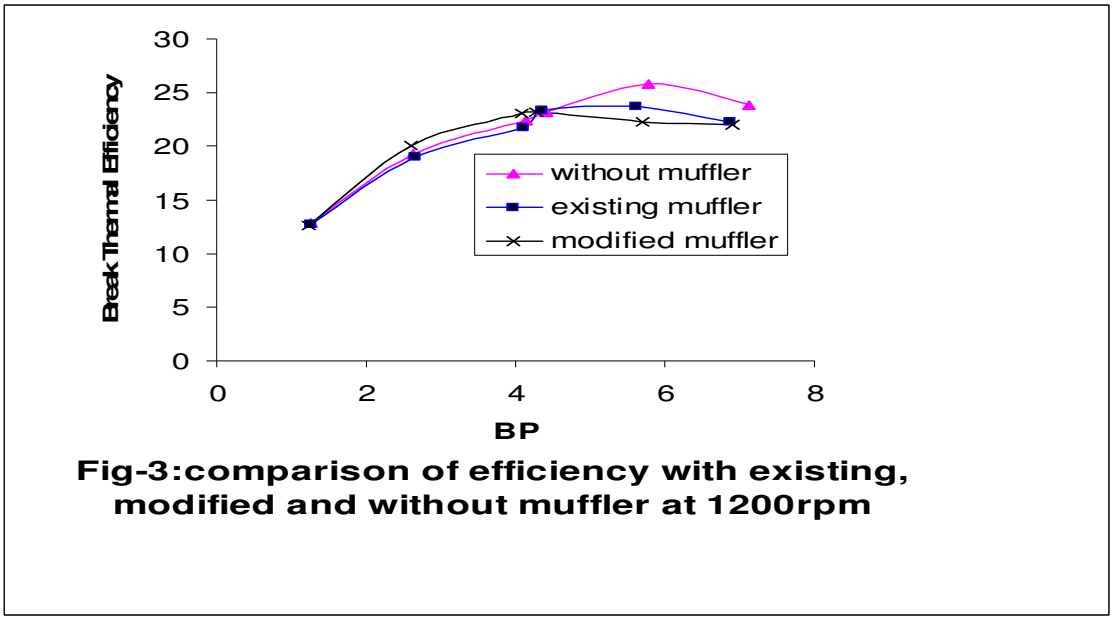

Fig-3:comparison of efficiency with existing, modified and without muffler at 1200rpm

From the result it is clear that the engine running at 1200 rpm, the performance is not so satisfactory with modified muffler. This is due to the low velocity of exhaust gas which causes separation of boundary layer giving pressure rises.

Figure 4 shows a graph of B.S.F.C Vs B.P. at 1200rpm. Minimum specific fuel consumption with modified muffler is 0.36 kg/ K watt which is 1.1% higher than existing muffler but 11.1% higher than the test result when engine was tested without muffler.

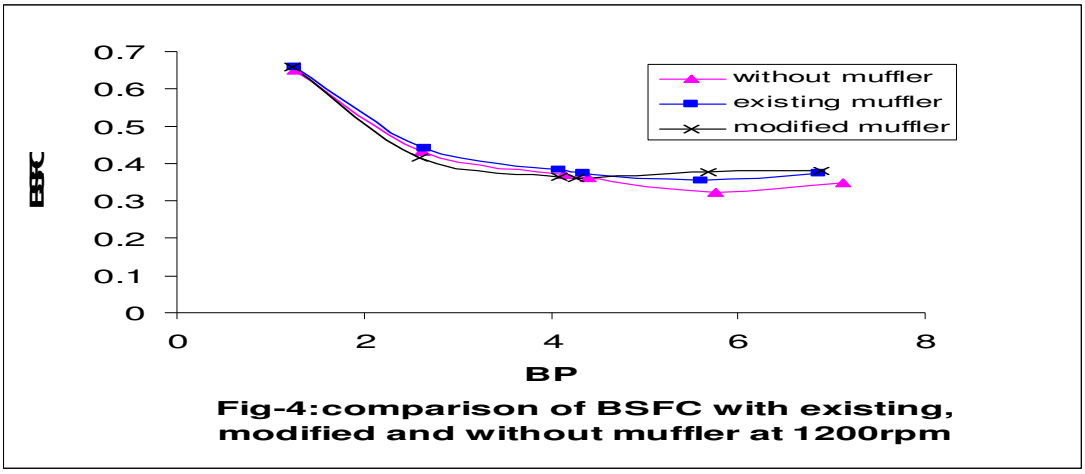

Fig-4:comparison of BSFC with existing, modified and without muffler at 1200rpm

The result is not supporting the modified muffler at 1200rpm. The break specific fuel consumption is higher compared with existing muffler which is caused by pressure rise in the reactive part of modified muffler due to boundary layer separation and reverse flow of exhaust. At this condition the residual burnt gas remains inside the cylinder which dilutes the fresh intake air which leads to incomplete combustion and low energy output from the fuel.

Figure 5 shows graph of η_{bth} Vs BP at 1300 rpm. The maximum break thermal efficiency of the engine modified muffler is 25.97% which is 1.8% higher than existing muffler and 0.33% lower than the performance of the engine when it was tested without muffler.

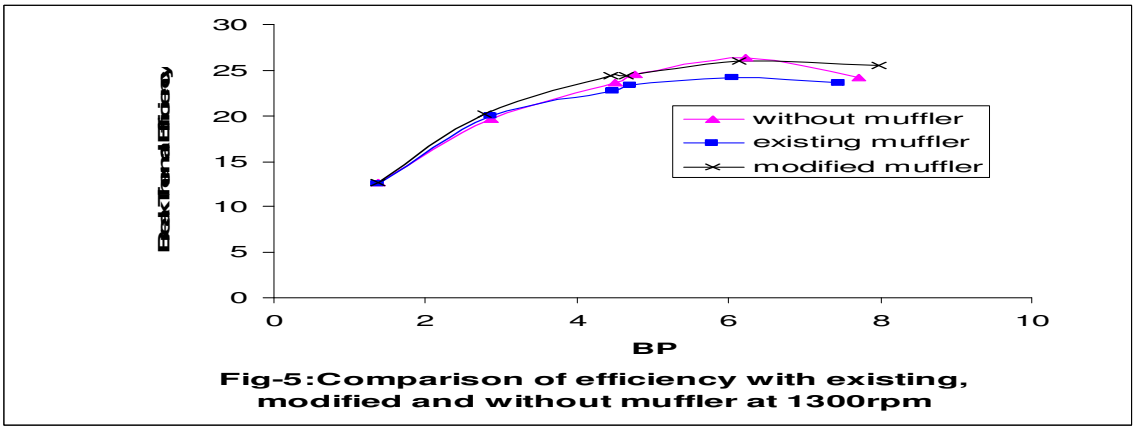

Fig-5:Comparison of efficiency with existing, modified and without muffler at 1300rpm

From above result it is clear that the engine is performing better with modified muffler. This is due to moderate velocity of exhaust gas which is free from boundary layer separation but overall performance of the engine is satisfactory at 1300 rpm.

Figure 6 shows a graph of B.S.F.C Vs B.P. at 1300rpm. Minimum specific fuel consumption with modified muffler is 0.322 kg/ K watt which is 7.5% lower than existing muffler but 0.63% higher than the test result when engine was tested without muffler. This is due to low pressure drop inside the reactive part of modified muffler as the flow is free from boundary layer separation and reverse flow.

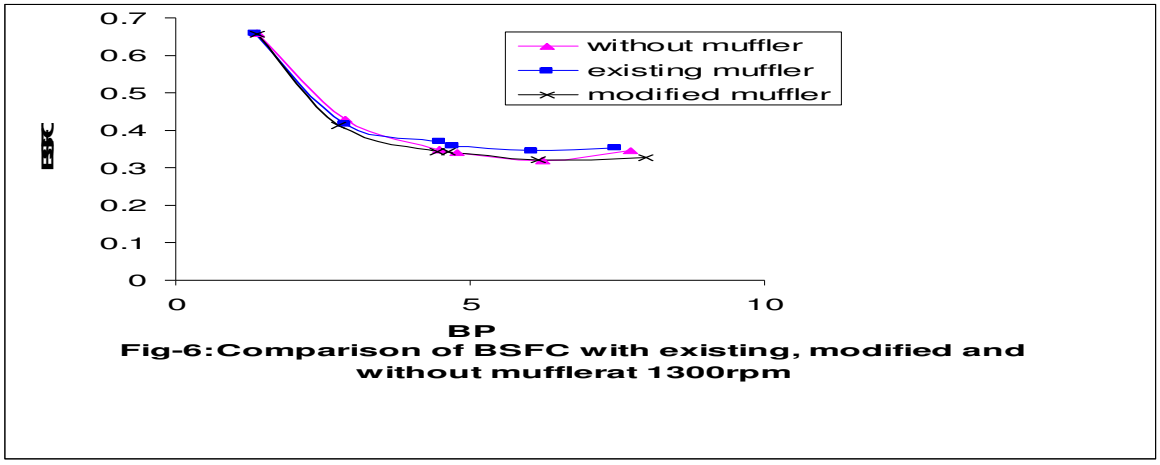

Fig-6:Comparison of BSFC with existing, modified and without mufflerat 1300rpm

From the result it is clear that the performance of the engine is better than the performance at 1200rpm. The result shows the better combustion when engine is running at 1300 rpm than 1200rpm.

Figure 7 shows graph of η_{bth} Vs BP at 1400 rpm. The maximum break thermal efficiency of the engine modified muffler is 26.24% which is 0.08% higher than existing muffler and 0.36% lower than the performance of the engine when it was tested without muffler.

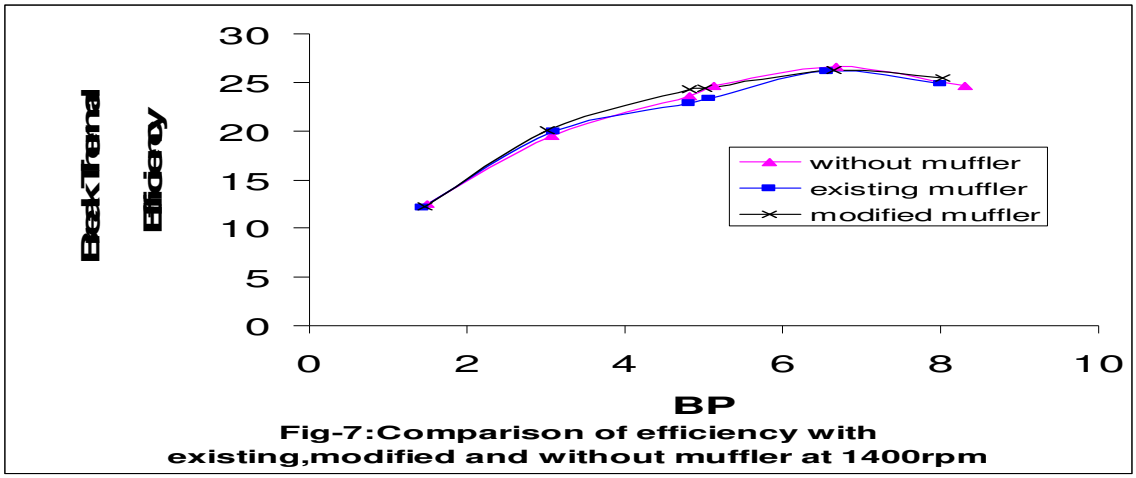

Fig-7:Comparison of efficiency with existing,modified and without muffler at 1400rpm

From the figure it is clear that engine is performing best with the modified muffler where the pressure drop due to modified muffler is negligibly small. This is due to simple configuration of the reactive part of modified muffler. There is minimum or almost no back flow of exhaust gas from muffler to engine.

Figure 8 shows a graph of B.S.F.C Vs B.P. at 1400rpm. As load increases fuel consumption increases as engine has to put more efforts for maintaining the speed. It is noted that B.S.F.C. decreases with increase in fuel consumption. Minimum specific fuel consumption with modified muffler is 0.32 kg/ K watt which is 0.4% lower than existing muffler but 1.9% higher than the test result when engine was tested without muffler. This due to same reason as explained earlier.

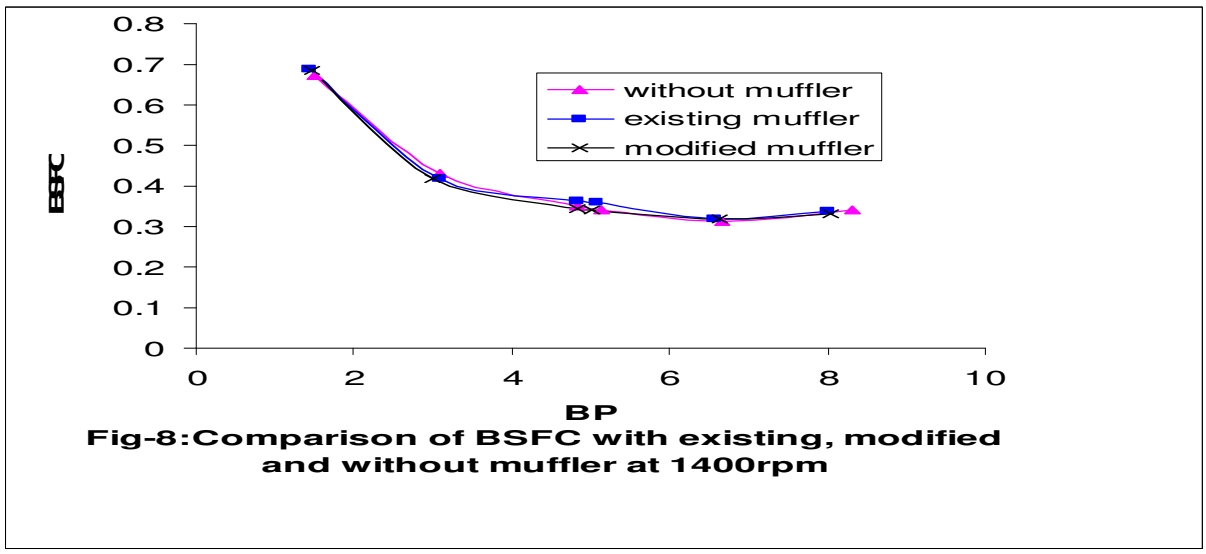

Fig-8:Comparison of BSFC with existing, modified and without muffler at 1400rpm

From the figure it is clear that the engine is giving better performance at 1400 rpm as compared with 1200 rpm and 1300rpm. It confirms the good combustion inside the engine and better recovery of energy from the combustion of fuel; as a result we are getting more mechanical energy from the engine.

Figure 9 shows graph of η_{bth} Vs BP at 1500 rpm. It is found that there is no considerable loss of power due to modified muffler. This is due to simple configuration of the muffler in which minimum back pressure is acting on the engine. The power loss due to back pressure is less. The maximum break thermal efficiency of the engine with modified muffler is 26.16% which is 0.72% higher than existing muffler and 0.67% lower than the performance of the engine when it was tested without muffler.

Fig-9:Comparison of efficiency with existing, modified and without muffler at 1500 rpm.

From the result it is clear that the efficiency of the engine is increasing at uniform rate at part loading but rate of increase of efficiency decreases at full loading with existing muffler as compared with the modified muffler because of low pressure drop leading to better combustion.

Figure 10 shows a graph of B.S.F.C Vs B.P. at 1500rpm. As load increases fuel consumption increases as engine has to put more efforts for maintaining the speed. It is noted that B.S.F.C. decreases with increase in fuel consumption. Minimum specific fuel

consumption with modified muffler is 0.321 kg/ K watt which is 2.8% lower than existing muffler but 3.5% higher than the test result when engine was tested without muffler.

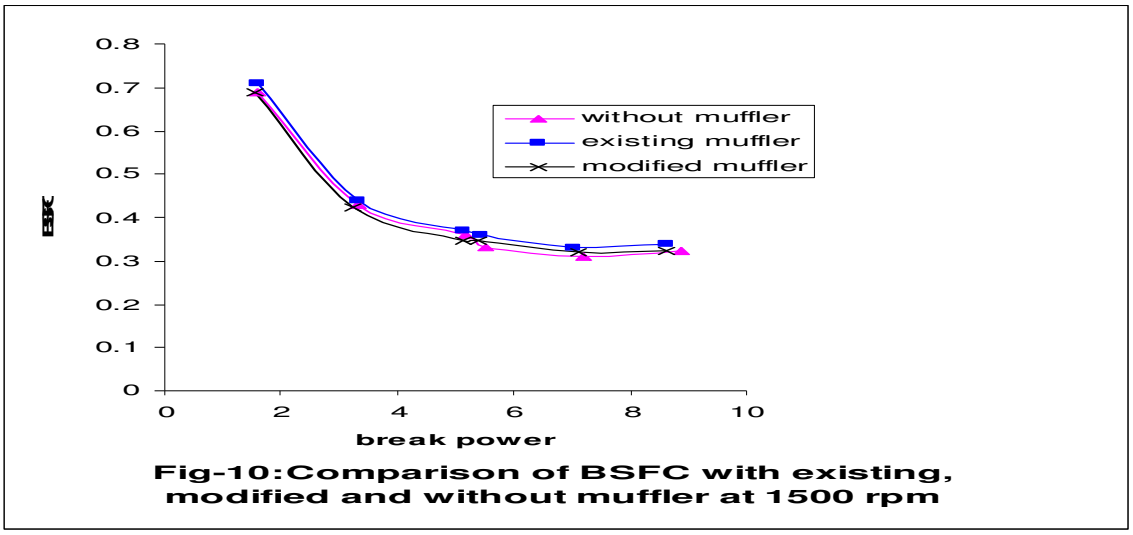

Fig-10:Comparison of BSFC with existing, modified and without muffler at 1500 rpm

From the result it is clear that the incomplete combustion occurs inside the engine during part load but gradually combustion improves with increase in load hence better performance of the engine.

From the results at different rpm it is clear that the performance of the engine is very good at 1400 rpm with modified muffler. Bellow 1400 rpm the performance of the engine becomes unsatisfactory.

Fig 11-14 represents the variation of sound level with respect to power output at different rpm. The sound pressure level increases with increase in load. At 1200 rpm with modified muffler the sound level is 14.5 db lower than existing muffler where as the sound level is 15.5 db lower at 1300rpm and 15.7db lower at 1400 rpm. At 1500 rpm with modified muffler the sound level is 14.7 db lower than existing muffler. From the above discussion it is clear that the modified muffler is effective at 1400 rpm. The sound pressure level by modified muffler is decreased considerably compared to the existing muffler because of decrease in pressure drop for simple configuration of modified muffler. The above mentioned plot will be useful to decide the maximum load at maximum speed of the engine for permissible S.P.L.

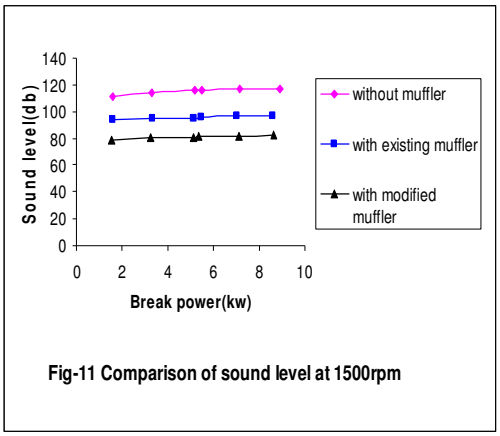

Fig-11 Comparison of sound level at 1500rpm

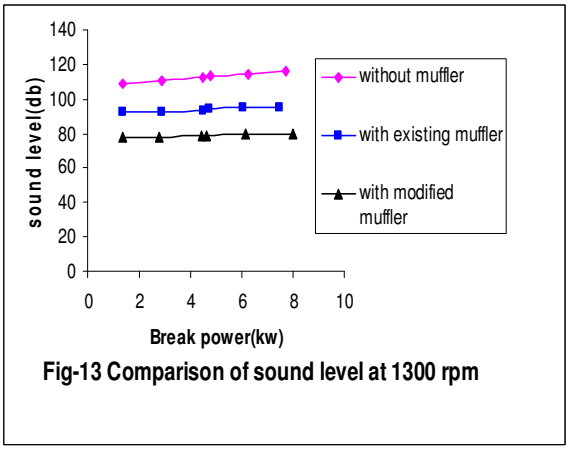

Fig-13 Comparison of sound level at 1300 rpm

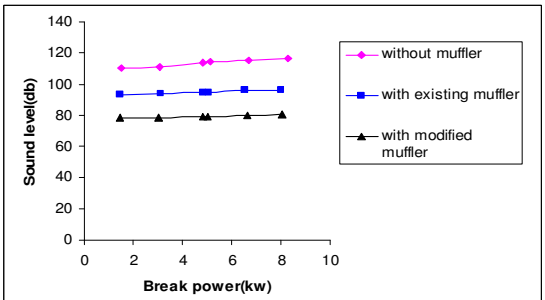

Fig-12 Comparison of sound level at 1400 rpm

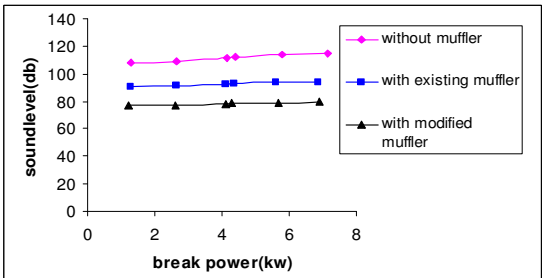

Fig-6.14 comparison of sound level at 1200 rpm

It has been observed that the engine performance curves with different mufflers are found to be very close to each other. The performance curves have been drawn as per the data generated which reflect the true engine performance having some uncertainty with measurement observations. However the performance obtained gives the true pictures with slight variation because of the possibility of measurement uncertainty.

Conclusion:

1) Sound level decreases 15dB approximately with modified muffler compared to existing muffler.

2) performance of all mufflers is comparable.

3) At 1400 rpm the modified muffler gives best result in comparison to the other mufflers.

Reference

[1] Prasad M.G. and Crocker M.J. *"Insertion loss studies on models of automotive exhaust systems"*, Journal of acoustical Society of America, Vol-70(5), pp. 1339-1334.

[2] Munjal, M.L. *"Acoustics of ducts and muffler with application to exhaust and ventilation system design"* 2nd edition , John Willy & Sons, N.Y. Ch 8,pp. 285-305.

[3] Munjal, M.L, Rao, K.N and Sahastrabudhe, A. D. *"Aero acoustic analysis of the two duct reverse flow perforated elements"*, Journal of Indian institute of science, 66, pp. 639-653.

[4] To, C.W.S. *"A note on various formulation for four pole parameters of a pipe with mean flow"*, Journal of sound and vibration, vol.88 (2), pp. 207-202.

[5] Thawani, Eriksson L.J., P.T. and Hoops, R.H. *"Acoustical design and evaluation of silencers"*, sound and vibration journals.

[6] Munjal, M.L. and Panicker, V.B. *"Radiation impedance of unplugged pipe with mean flow"*, Noise control engineering, 18(2), pp. 48-51.

[7] Sullivan, J.W. *"Modeling of engine exhaust system noise"*, Noise and fluid engineering proceeding of winter annual meeting of ASME (Atlanta), pp.161-169.

[8] Chang I. J. and Cummings A. *" A time domain solution for attenuation at high amplitudes of perforated tube silencers and comparison with experiments"* Journal of Sound and Vibration , 122(2), pp. 1-17.

[9] Davies, P.O.A.L. *"Flow acoustic coupling in ducts"* Journal of Sound and Vibration, 77(2), pp. 191-209

[10] Bankim Bihari Ghosh, Rajsekhar Panua, Paritosh Bhattacharya Prabir Kumar Bose. "*Analytical and experimental study on noise attenuation of multi-cylinder*

diesel engine with resonative muffler" Journal of Applied Sciences Research, 3(8): 676-680, 2007© 2007, INSInet Publication.

[11] Bankim Bihari Ghosh, Rajsekhar Panua, Paritosh Bhattacharya Prabir Kumar Bose. "*Prediction of noise level by mathematical modeling in the exhaust muffler and validation of these analytical results with the experimental results for 4-stroke diesel engine"* Jouranl of Advances in Applied Mathematical Analysis (AAMA)Volume 2 Number 1 (2007) pp. 41-49.